

Sample size and power calculation for propensity score analysis of observational studies

Bo Liu

Department of Statistical Science, Duke University

and

Xiaoxiao Zhou

Department of Biostatistics, The University of Alabama at Birmingham

and

Fan Li

Department of Statistical Science, Duke University

January 29, 2025

Abstract

This paper develops theoretically justified analytical formulas for sample size and power calculation in the propensity score analysis of causal inference using observational data. By analyzing the variance of the inverse probability weighting estimator of the average treatment effect (ATE), we clarify the three key components for sample size calculations: propensity score distribution, potential outcome distribution, and their correlation. We devise analytical procedures to identify these components based on commonly available and interpretable summary statistics. We elucidate the critical role of covariate overlap between treatment groups in determining the sample size. In particular, we propose to use the Bhattacharyya coefficient as a measure of covariate overlap, which, together with the treatment proportion, leads to a uniquely identifiable and easily computable propensity score distribution. The proposed method is applicable to both continuous and binary outcomes. We show that the standard two-sample z -test and variance inflation factor methods often lead to, sometimes vastly, inaccurate sample size estimates, especially with limited overlap. We also derive formulas for the average treatment effects for the treated (ATT) and overlapped population (ATO) estimands. We provide simulated and real examples to illustrate the proposed method. We develop an associated R package `PSpower`.

Keywords: causal inference, observational study, overlap, power, sample size, weighting

1 Introduction

Randomized controlled trials are the gold standard for causal inference, but they are not always feasible due to logistical or ethical constraints. Researchers are increasingly using observational data to emulate randomized trials. Designing randomized or emulated trials requires sample size and power calculations. In these calculations, investigators pre-specify a target estimand—typically the effect size of a treatment—and characteristics of the sample in the intended study. The goal of sample size calculation is to determine the minimal sample size needed to achieve the statistical power $(1 - \beta)$, given a type I error rate (α) level, in testing the treatment effect estimated by a specific method based on a sample that satisfies these characteristics. Conversely, the goal of power calculation is to determine the power in detecting a treatment effect at the α level given a fixed sample size. Sample size and power calculations are the two sides of the same coin; for simplicity, henceforth we will refer to both as sample size calculation.

Sample size calculation is conducted in the design stage of a study, prior to data collection. Thus, individual data are usually unavailable; investigators at best have some summary information of previous similar studies, e.g. mean and variances of covariates and outcomes by treatment arm. Lack of individual data renders sample size calculation challenging: analysts must rely on limited summary information of the intended study to approximately recover the full data structure. One exception is randomized trials, where the sample size calculation is much simplified. The primary difference between randomized trials and observational studies is confounding. Randomized trials have no confounding by design; therefore, one can simply use the difference in the mean outcomes between arms to estimate the treatment effects. Closed-form formulas, e.g., based on the two-sample z-test, are readily applicable for sample size calculation. In contrast, in observational studies,

confounding must be adjusted to obtain an unbiased estimate of treatment effects. The existing literature on sample size calculation has largely focused on randomized studies. The current common practice is to apply sample size calculation formulas designed for randomized trials to observational studies. As we shall show later, this practice often leads to, sometimes vastly, underpowered studies.

Some authors have used the variance inflation factor or design effects (Hsieh and Lavori, 2000; Scosyrev and Glimm, 2019; Shook-Sa and Hudgens, 2022; Austin, 2021) to approximate the potential inflation in the sample size of an observational study compared to a randomized trial. However, such methods lack theoretical foundation; more importantly, as we will show later, they often lead to inaccurate estimates. Other methods use simulations to generate individual data based on pre-specified summary statistics (Qin, 2024), but there is no theoretical basis on what summary statistics are adequate. In fact, many different data generating models may satisfy the same summary statistics but lead to vastly different sample sizes; choosing between these models is usually *ad hoc*. Motivated by the gap, we rigorously investigate the power and sample size calculation for causal inference in observational studies. We focus on the widely used propensity score methods (Rosenbaum and Rubin, 1983), which use propensity scores to create covariate balance between treatment groups and thus emulate a target randomized trial. Despite the extensive literature on propensity score methods, there is no discussion on related sample size calculation. With limited prior information, the central task in sample size calculation is to parsimoniously specify a set of easily available summary statistics from previous studies that are sufficient to robustly determine the variance of a given causal estimator. Other criteria in selecting these conditions are interpretability and computation. Based on the analysis of variance of the common Hájek weighting estimator, we will pro-

vide a set of summary statistics and associated sample size and power calculation formulas that satisfy these criteria. We derive analytical formulas for three common causal estimands: the average treatment effect for the overall (ATE), treated (ATT), and overlapped population (ATO). We develop an associated R package `PSpower`, available on CRAN at <https://CRAN.R-project.org/package=PSpower>.

2 Variance and sample size based on the Hájek estimator

Suppose we have a sample of N units. Each unit i ($i = 1, 2, \dots, N$) has a binary treatment indicator Z_i , with $Z_i = 0$ being the control and $Z_i = 1$ being treated, and a vector of p covariates $X_i = (X_{1i}, \dots, X_{pi})'$. Assuming the Stable Unit Treatment Value Assumption (SUTVA), for each unit i , there is a pair of potential outcomes $\{Y_i(1), Y_i(0)\}$ mapped to the treatment and control status, of which only the one corresponding to the observed treatment is observed, denoted by $Y_i = Z_i Y_i(1) + (1 - Z_i) Y_i(0)$; the other potential outcome is counterfactual. The propensity score is the probability of a unit being assigned to the treatment group given the covariates (Rosenbaum and Rubin, 1983): $e(x) = \Pr(Z_i = 1 | X_i = x)$.

The goal is to use the sample to estimate the average treatment effect (ATE):

$$\tau = \mathbb{E}[Y_i(1) - Y_i(0)] = \mathbb{E}_x[\tau(x)], \tag{1}$$

where $\tau(x) = \mathbb{E}[Y_i(1) - Y_i(0) | X_i = x]$ is the conditional average treatment effect (CATE) at covariate value x . To identify the ATE, we usually make the strong ignorability assumption, consisting of two sub-assumptions: (i) unconfoundedness, $\Pr(Z_i | Y_i(0), Y_i(1), X_i) = \Pr(Z_i | X_i)$; (ii) overlap, i.e. $0 < \Pr(Z_i | X_i) < 1$. Under strong ignorability and overlap,

we can identify the ATE from the observed data as $\tau = \mathbb{E}[Y_i Z_i / e(X_i)] - \mathbb{E}[Y_i(1 - Z_i) / (1 - e(X_i))]$. Among the consistent estimators of ATE, we focus on the Hájek inverse probability weighting (IPW) estimator for analytical simplicity:

$$\hat{\tau}_N = \frac{\sum_{i=1}^N Y_i Z_i / e(X_i)}{\sum_{i=1}^N Z_i / e(X_i)} - \frac{\sum_{i=1}^N Y_i(1 - Z_i) / [1 - e(X_i)]}{\sum_{i=1}^N (1 - Z_i) / [1 - e(X_i)]}. \quad (2)$$

Lunceford and Davidian (2004) show that $\sqrt{N}(\hat{\tau}_N - \tau)$ is asymptotically normal with variance

$$V = \mathbb{E} \left[\frac{\{Y(1) - \mathbb{E}[Y(1)]\}^2}{e(X)} \right] + \mathbb{E} \left[\frac{\{Y(0) - \mathbb{E}[Y(0)]\}^2}{1 - e(X)} \right]. \quad (3)$$

In observational studies, the true propensity score is unknown and is replaced by an estimated one. Lunceford and Davidian (2004) show that the asymptotic variance of the Hájek estimator with estimated propensity score, V_0 , is V subtracted by a complex quadratic term and therefore smaller. Calculation of the quadratic term usually requires individual data, which is unavailable in most sample size calculation. Therefore, we will proceed with V henceforth, noting that it leads to a conservative (i.e. larger) sample size estimate than that based on V_0 . The discrepancy between V and V_0 depends on (i) how imbalanced the covariates between two groups are, and (ii) how predictive the covariates are of the outcome. The intuition is analogous to that underlying the efficiency gain using estimated versus true propensity scores in estimating the ATE with covariate adjustment in randomized experiments (Shen et al., 2014). We will investigate this discrepancy using simulations in Section 5.

With a fixed value of V , a $(1 - \alpha)$ confidence interval for $\hat{\tau}_N$ is $\hat{\tau}_N \pm z_{1-\alpha/2} V^{1/2} N^{-1/2}$, where $z_{1-\alpha/2}$ is the $(1 - \alpha/2)$ quantile of the standard normal distribution. Without loss of generality, we consider an one-sided level- α hypothesis test for the null $H_0 : \tau = 0$ against the alternative $H_a : \tau > 0$:

$$\text{reject } H_0 \text{ if } \hat{\tau}_N > z_{1-\alpha} \sqrt{V/N}. \quad (4)$$

The following proposition establishes the minimal sample size N to reach a desired power β for a level- α test (4) (the proof is relegated to Appendix A.1).

Proposition 1. *Let $\beta \geq 0.5 \geq \alpha$ be the required power of the test (4). Then, the relationship between the sample size N and power β is*

$$N = \frac{\left(z_{1-\alpha}\sqrt{V} - z_{1-\beta}\sqrt{V_0}\right)^2}{\tau^2} \leq \frac{V}{\tau^2} (z_{1-\alpha} + z_\beta)^2. \quad (5)$$

In a randomized experiment, the propensity score is fixed and known, e.g. in a balanced design $e(X) = 0.5$, so that V simplifies to $2\{\mathbb{V}[Y(1)] + \mathbb{V}[Y(0)]\}$. Moreover, $\Pr(Y(z)) = \Pr(Y | Z = z)$, and thus variance of the potential outcomes $Y(z)$ can be directly estimated by the sample variances of the outcome in arm z , s_z^2 . Therefore, to detect a treatment effect τ in a balanced randomized experiment using a one-sided level- α test (4) with power β , the minimal sample size is

$$N = \frac{2(s_1^2 + s_0^2)}{\tau^2} (z_{1-\alpha} + z_\beta)^2. \quad (6)$$

This coincides with the standard sample size formula of a two-sample z -test.

In observational studies, sample size calculation is more complicated because (i) the propensity scores $e(X)$ are not known, (ii) generally $\Pr(Y(z)) \neq \Pr(Y | Z = z)$ due to confounding, and thus the terms involving potential outcomes, such as $\mathbb{E}[Y(z)]$ and $\mathbb{V}[Y(z)]$, deviate from their observed counterparts $\mathbb{E}[Y | Z = z]$ and $\mathbb{V}[Y | Z = z]$, and (iii) the numerator and denominator inside the expectation operator in (3) can not be separated because the potential outcomes may be dependent of the propensity scores. When sampled units are available, we can readily address these complications. However, sample size calculation is conducted prior to data collection, with little information to either estimate the propensity scores or calculate the expectations directly. Nonetheless, analysts usually have some summary information from historical studies about the intended population.

The next section will develop an approach for sample size calculation based on standard available summary statistics.

3 Sample size calculation

The essence of sample size calculation lies in computing the variance V in (3). If we could observe (X_i, Z_i, Y_i) for each sampled unit i , V could easily be estimated by sample moments, but not so with only summary data. To determine which summary information is sufficient for computing V , we rewrite the terms in expression (3) as (taking $z = 1$ for example),

$$\mathbb{E} \left[\frac{\{Y(1) - \mathbb{E}[Y(1)]\}^2}{e(X)} \right] = \mathbb{E} [\{Y(1) - \mathbb{E}[Y(1)]\}^2] \mathbb{E} \left[\frac{1}{e(X)} \right] + \text{Cov} \left[\{Y(1) - \mathbb{E}[Y(1)]\}^2, \frac{1}{e(X)} \right]. \quad (7)$$

This expression suggests that we need three components: (i) mean and variance of the potential outcome in each arm, (ii) mean of (the inverse of) the propensity score, and (iii) covariance between the potential outcomes and propensity score. We study each of the components in detail below.

3.1 Normal approximation of covariates

Both the propensity score and the outcome models are commonly specified as a generalized linear model with a linear combination of the covariates, $X'\beta = \sum_{j=1}^p \beta_j X_j$ as the predictor. However, in sample size calculation, we usually do not have either individual data or even summary statistics of each covariate, without which we cannot characterize the distributions of the propensity score or the outcome. Previous authors often operated with a single normal predictor (e.g. Raudenbush, 1997; Kelcey et al., 2017; Qin, 2024), but without theoretical justification. Here we present a special case of the Lyapunov Central Limit

Theorem (Billingsley, 1995) to approximate the distribution of the scalar summary $X'\beta$ and thus justify such a procedure.

Theorem 1. *Assume X_1, X_2, \dots is a sequence of independent random variables with mean 0 and variance 1. Let β_1, β_2, \dots be a sequence of real numbers. If the following two conditions hold: (i) there exists a positive number B such that $\mathbb{E}[X_j^4] < B$, and (ii) $\max_{1 \leq j \leq p} \frac{\beta_j^2}{\sum_{j=1}^p \beta_j^2} = o(1)$, then*

$$\frac{1}{\sum_{j=1}^p \beta_j^2} \sum_{j=1}^p \beta_j X_j \Rightarrow \mathbf{N}(0, 1). \quad (8)$$

The proof of Theorem 1 is relegated to Appendix A.2. Condition (i) ensures that the distribution of each covariate does not have heavy tails, and condition (ii) ensures that no single covariate dominates the linear combination. Though these two conditions may not always hold, empirical evidence from simulated and three real applications (see Appendix B.1) shows the normality generally holds in a wide range of scenarios.

3.2 Distribution of propensity scores

The propensity score is usually specified by a logistic regression model: $e(X) = \text{expit}(W_e)$, where $W_e = \beta_0 + \sum_{j=1}^p \beta_j X_j$. Theorem 1 motivates us to approximate the distribution of the scalar summary W_e by a normal distribution $\mathbf{N}(\mu_e, \sigma_e^2)$, and thus approximate the propensity score distribution by a logit-normal distribution $\mathcal{P}(\mu_e, \sigma_e^2)$.

To determine the two parameters μ_e and σ_e of the logit-normal distribution, we would need to impose constraints in the form of summary information of the treatment assignment. The first constraint, which is nearly always available, is the proportion of the treatment group in the intended study: $r = \Pr(Z_i = 1)$. The second constraint is a measure, denoted as ϕ , of the similarity between the covariate distributions in the treatment and control groups, $\Pr(X | Z = 1)$ versus $\Pr(X | Z = 0)$. There are many choices of the specification

of ϕ ; important selection criteria include: (i) there should be 1-1 map between (r, ϕ) and (μ_e, σ_e) so that the data generating process of the propensity score is unique, and (ii) easy to compute the propensity score distribution (equivalently μ_e, σ_e) given (r, ϕ) .

The logit-normal distribution does not have a closed-form mean and thus it is generally difficult to solve for (μ_e, σ_e) given (r, ϕ) . Instead, we propose to approximate the logit-normal distribution by a Beta distribution, which has a range on $[0, 1]$ and is easy to compute. Applying the method in Aitchison and Shen (1980), we can derive the “optimal” Beta function approximation of a logit-normal function by minimizing the Kullback-Leibler divergence between them. Specifically, for a logit-normal distribution $\mathcal{P}(\mu_e, \sigma_e^2)$ and its optimal approximated Beta distribution $\text{Beta}(a, b)$, their parameters must satisfy the following relation: $\mu_e = \psi(a) - \psi(b)$ and $\sigma_e^2 = \psi'(a) + \psi'(b)$, where ψ and ψ' are the digamma and trigamma functions, respectively. Numerical examples in Appendix B.2 illustrate that this approximation is accurate for a wide range of logit-normal distributions.

If $e(X) \sim \text{Beta}(a, b)$, then there is a closed-form relation between a, b, r :

$$r = \frac{a}{a + b}. \quad (9)$$

Therefore, it suffices to identify the propensity score distribution if we find another easily computable relation between a, b and the overlap measure ϕ . The question now becomes how to specify such a ϕ . Directly operating on the multivariate covariate X is challenging; instead we operate on the propensity score $e(X)$, which is the coarsest balancing score (Rosenbaum and Rubin, 1983). Let $f_z(u)$ be the density of the propensity score in arm z : $f_z(u) = \Pr(e(X) = u \mid Z = z)$. We propose to use the Bhattacharyya coefficient (Bhattacharyya, 1943) to measure the covariate overlap between two groups:

$$\phi \equiv \int_0^1 \sqrt{f_1(u)f_0(u)} \, du. \quad (10)$$

The Bhattacharyya coefficient ϕ satisfies $0 \leq \phi \leq 1$, with $\phi = 0$ if and only if the support of f_0 and f_1 does not overlap, whereas $\phi = 1$ if and only if $f_0 = f_1$ almost everywhere. Therefore, ϕ is an appropriate measure of overlap; we term it as the *overlap coefficient* hereafter. We choose the Bhattacharyya coefficient because it has a major computable advantage in our context, established in the following proposition (the proof is relegated to Appendix A.3).

Proposition 2. *For $e(X) \sim \text{Beta}(a, b)$, the overlap coefficient ϕ has a closed-form expression as a function of (a, b) :*

$$\phi = \frac{\Gamma(a + 0.5) \Gamma(b + 0.5)}{\sqrt{a}\Gamma(a) \sqrt{b}\Gamma(b)}. \quad (11)$$

Therefore, given (r, ϕ) , we can obtain the Beta parameters (a, b) by solving for Equation (9) and (11). Specifically, based on Equation (9), it is natural to reparameterize (a, b) as $a = kr$ and $b = k(1 - r)$, under which Equation (11) becomes

$$\phi(k) = \frac{\Gamma(kr + 0.5) \Gamma(k(1 - r) + 0.5)}{\sqrt{kr}\Gamma(kr) \sqrt{k(1 - r)}\Gamma(k(1 - r))}. \quad (12)$$

We write $\phi(k)$ to highlight that, given r , the overlap coefficient ϕ is a function of the unknown k . The following proposition establishes that, given r , there is a 1-1 map between ϕ and k , and equivalently, a 1-1 map between (r, k) and (a, b) . The proof is relegated to Appendix A.4.

Proposition 3. *The function, $\phi(k)$, defined in (12), is monotonically increasing in k if $k > \max\left\{\frac{1}{2r}, \frac{1}{2(1-r)}\right\}$.*

Proposition 3 allows us to use the bisection method to solve for k efficiently. Interestingly, our experience suggests that many other specification of the overlap coefficient do not lead to a 1-1 map to the propensity score distribution. In summary, as long as users specify (r, ϕ) , we can solve for the Beta parameters (a, b) in a computationally efficient

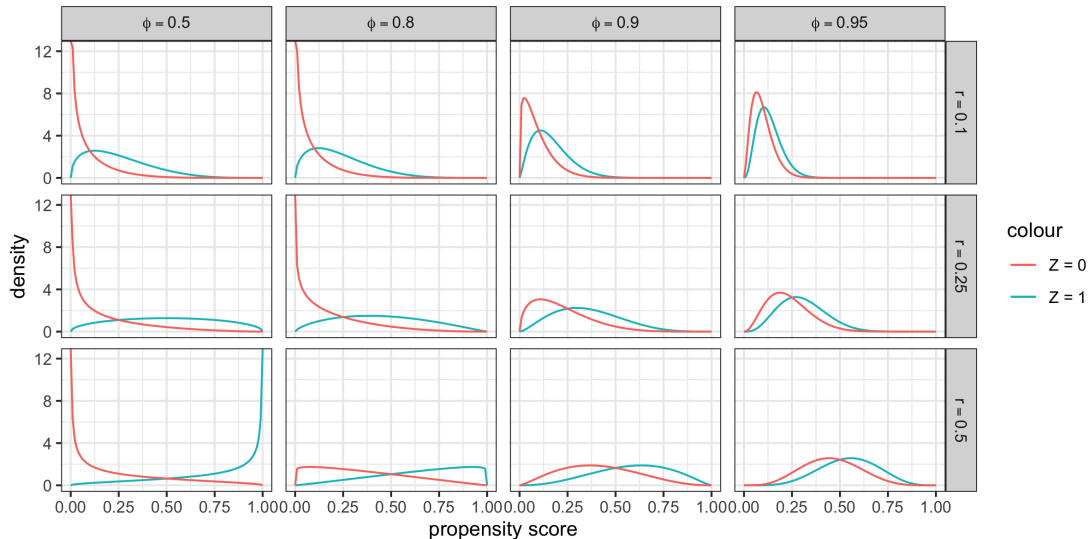


Figure 1: Distributions of $e(X)$ versus $1 - e(X)$ corresponding to different combinations of (r, ϕ) , where $e(X)$ follows a $\text{Beta}(a, b)$ distribution with a and b determined by (r, ϕ) .

fashion, based on which we further reverse the Beta approximation of $e(X)$ to obtain the logit-normal distribution parameters (μ_e, σ_e) .

To visualize the overlap coefficient, Figure 1 shows the distributions of $e(X)$ versus $1 - e(X)$ corresponding to different combinations of (r, ϕ) . In practice, we recommend users to combine substantive knowledge with Figure 1 to provide a reasonable input of ϕ given r . For example, as a generic rule of thumb for a balanced design with $r = 0.5$, we recommend to code $\phi = (0.9, 0.8, 0.5)$ as good, medium, and poor overlap, respectively.

3.3 Distribution of potential outcomes

For simplicity, we first focus on continuous outcomes. The potential outcomes are usually specified as a linear model $Y(z) = \gamma_{z0} + X'\gamma_z + \epsilon_z$, with $\mathbb{E}[\epsilon_z] = 0$. Similarly as before, Theorem 1 motivates us to approximate the distribution of $X'\gamma_z$ by a normally distributed random variable W_z .

Recall that we approximated the distribution of the propensity score by $e(X) = \text{expit}(W_e)$,

where $W_e \sim \mathbf{N}(\mu_e, \sigma_e^2)$ is a normal random variable. Therefore, the correlation between the potential outcomes and the propensity score is captured by the correlation between W_e and W_z . This motivates us to decompose W_z into two parts, one linear in W_e and the other orthogonal to W_e . Specifically, we can decompose $W_z = a_z W_e + W_e^\perp$ such that $\text{cov}(W_e, W_e^\perp) = 0$. Then, the potential outcomes can be expressed as $Y(z) = a_z W_e + W_e^\perp + \epsilon_z$, where both W_e^\perp and ϵ_z are unknown normal random variables. Because both variables are independent of W_e , it is impossible to further identify W_e^\perp from ϵ_z ; thus, with slight abuse of notation, we combine these two terms and denote the sum as ϵ_z , under which the potential outcomes are modeled as

$$Y(z) = a_z W_e + \epsilon_z, \quad \epsilon_z \sim \mathbf{N}(\mu_z, \sigma_z^2). \quad (13)$$

Here we have six unknown parameters in total to characterize the potential outcome distributions: $a_1, a_0, \mu_1, \mu_0, \sigma_1^2, \sigma_0^2$. In sample size calculation settings, users usually have prior knowledge of the mean and variance of the observed outcome in each treatment group (e.g. available in Table 1 of a previous study in medical papers), denoted as $E_z \equiv \mathbb{E}[Y \mid Z = z]$ and $S_z \equiv \mathbb{V}[Y \mid Z = z]$, for $z = 0, 1$. These are different from their counterparts to the potential outcomes $\mathbb{E}[Y(z)]$ and $\mathbb{V}[Y(z)]$. In addition to these four quantities, we would need two more constraints to identify the six parameters; it is natural to use the correlation between the covariates and the observed outcomes, i.e., $R_z \equiv \text{cor}[Y, W_e \mid Z = z]$. We postpone the detailed discussion of R_z to Section 3.4.

With the six specified values $(E_1, E_0, S_1, S_0, R_1, R_0)$, one can solve for the unknown parameters $(a_1, a_0, \mu_1, \mu_0, \sigma_1^2, \sigma_0^2)$ by the following equations (the proof is relegated to Appendix A.5)

$$a_z = R_z \sqrt{\frac{S_z}{\mathbb{V}[W_e \mid Z = z]}}, \quad \mu_z = E_z - a_z \mathbb{E}[W_e \mid Z = z], \quad \sigma_z^2 = (1 - R_z^2) S_z. \quad (14)$$

Note that the conditional mean $\mathbb{E}[W_e \mid Z = z]$ and variance $\mathbb{V}[W_e \mid Z = z]$ do not have

closed forms. We propose to calculate them numerically by the following formula

$$\mathbb{E}[W_e | Z = z] = \frac{\int_{\mathbb{R}} x \exp\left\{-\frac{1}{2\sigma_e^2}(x - \mu_e)^2\right\} \text{expit}\{(-1)^{1-z}x\} dx}{\int_{\mathbb{R}} \exp\left\{-\frac{1}{2\sigma_e^2}(x - \mu_e)^2\right\} \text{expit}\{(-1)^{1-z}x\} dx}, \quad (15)$$

$$\mathbb{V}[W_e | Z = z] = \frac{\int_{\mathbb{R}} x^2 \exp\left\{-\frac{1}{2\sigma_e^2}(x - \mu_e)^2\right\} \text{expit}\{(-1)^{1-z}x\} dx}{\int_{\mathbb{R}} \exp\left\{-\frac{1}{2\sigma_e^2}(x - \mu_e)^2\right\} \text{expit}\{(-1)^{1-z}x\} dx} - (\mathbb{E}[W_e | Z = z])^2. \quad (16)$$

Once the parameters $(a_1, a_0, \mu_1, \mu_0, \sigma_1^2, \sigma_0^2)$ are solved, we can fully determine the distribution of $Y(0)$ and $Y(1)$.

3.4 Correlation between outcomes and covariates

The correlation parameter $R_z = \text{cor}[Y, W_e | Z = z]$ may be challenging to interpret and specify. We first give an intuitive explanation. In observational studies, only the observed mean outcomes $\mathbb{E}[Y | Z = z]$, instead of the target potential outcomes $\mathbb{E}[Y(z)]$, are observable. If R_z deviates far from zero, meaning that the covariates that are correlated with the propensity score are also correlated with the potential outcome, then $\mathbb{E}[Y(z)]$ would be more likely different from $\mathbb{E}[Y | Z = z]$ because the units in the opposite treatment group would likely have different covariates that lead to different potential outcomes. Therefore, as R_z increases, larger sample sizes are needed to recover the counterfactual $\mathbb{E}[Y(z)]$ from the observed $\mathbb{E}[Y | Z = z]$.

To gain more technical insight into R_z , consider the simple setting in which all covariates are uncorrelated and standardized with mean 0 and variance 1 within each treatment arm, *i.e.*, $\mathbb{V}[X | Z = z] = I_p$, where I_p is an identity matrix of dimension p . Recall that the propensity score and the outcome models are $e(X) = \text{expit}(\beta_0 + X'\beta)$ and $Y(z) = \gamma_{z0} + X'\gamma_z + \epsilon_z$, respectively. In this outcome model, the variance of $Y(z)$ can be decomposed into two components, $\mathbb{V}[X'\gamma_z | Z = z]$ and $\mathbb{V}[\epsilon_z | Z = z]$, respectively.

The first component originates from the variance of X and can be explained by the individual covariates. The second component is the unexplainable variance introduced by ϵ_z . Thus, these two components are often termed signal and noise, respectively. We define $\text{SNR}_z = \mathbb{V}[X'\gamma_z | Z = z]/\mathbb{V}[\epsilon_z | Z = z]$ as the signal-to-noise ratio of the outcome model. Then the correlation parameter

$$R_z = \frac{\beta'\gamma_z}{\sqrt{\beta'\beta \cdot (\gamma_z'\gamma_z + \mathbb{V}[\epsilon_z | Z = z])}} = \frac{\cos\langle\beta, \gamma_z\rangle}{\sqrt{1 + \text{SNR}_z^{-1}}}, \quad (17)$$

where the numerator $\cos\langle\beta, \gamma_z\rangle$ is the cosine of the angle between β and γ_z , which measures the closeness in direction of the coefficients β and γ_z . When the sets of covariates associated with the propensity scores and the potential outcomes, respectively, are distinct, β and γ_z are close to orthogonal, and thus $\cos\langle\beta, \gamma_z\rangle$ will be close to 0. This includes randomized experiments as a special case. In general cases, the angle can be obscure for researchers; nevertheless, the absolute value of R_z is bounded by $1/\sqrt{1 + \text{SNR}_z^{-1}}$, or $\sqrt{\text{SNR}_z}$ when SNR_z is small. The signal-to-noise ratio, SNR_z , does not involve propensity scores; instead, it only measures how much variation in the outcomes can be explained by the covariates and is arguably easier to specify than R_z .

The expression of R_z does not depend on the intercepts β_0 and γ_{z0} . Therefore, R_z is invariant under transformation of the potential outcome models. Specifically, under homogeneous effects $Y(1) = Y(0) + \tau$, we always have $R_1 = R_0$; under heterogeneous effects, simulations and real applications in Section 5 suggest that R_1 and R_0 are often similar. Thus, to simplify the implementation, we recommend to impose $R_1 = R_0 = R$ and treat R as a sensitivity parameter. As shown in (19) and (24), the sample size formulas for both ATE and WATE depend only on the absolute value of R . Therefore, the range of R can be reduced to $[0, \sqrt{\text{SNR}_z}]$ instead of $[-1, 1]$.

3.5 Analytical formula for sample size calculation

Summarizing the building blocks in Section 3.2-3.4, we propose to approximate the distribution of the propensity score and the potential outcomes as

$$e(X) = \text{expit}(W_e), \quad Y(z) = a_z W_e + \epsilon_z, \quad W_e \sim \mathbf{N}(\mu_e, \sigma_e^2), \quad \epsilon_z \sim \mathbf{N}(\mu_z, \sigma_z^2), \quad (18)$$

respectively, where the propensity score model parameters (μ_e, σ_e) and the outcome model parameters $(a_1, a_0, \mu_1, \mu_0, \sigma_1^2, \sigma_0^2)$ can be uniquely determined by the user specified inputs (r, ϕ) and $(r, \phi, E_1, E_0, S_1, S_0, R_1, R_0)$, respectively. The following theorem presents the analytical formula for the sample size calculation of the ATE (the proof is relegated to Appendix A.6).

Theorem 2. *Let τ be the desired effect size of the ATE. The minimum sample size for a two-sided level- α test (4) for detecting τ with power β is $N = V (z_{1-\alpha/2} + z_\beta)^2 / \tau^2$, where*

$$\begin{aligned} V = & (a_1^2 + a_0^2) \sigma_e^2 + (\sigma_1^2 + \sigma_0^2) + [a_1^2 \sigma_e^2 (\sigma_e^2 + 1) + \sigma_1^2] \exp(-\mu_e + \sigma_e^2/2) \\ & + [a_0^2 \sigma_e^2 (\sigma_e^2 + 1) + \sigma_0^2] \exp(\mu_e + \sigma_e^2/2). \end{aligned} \quad (19)$$

Remark 1. The above analytical derivation elucidates the critical role of covariate overlap in sample size calculations of observational studies. Specifically, the overlap coefficient ϕ explicitly determines the propensity score distribution, which in turn determines the potential outcome distributions because of the projection of $Y(z)$ on W_e . Intuitively, as the overlap decreases, the observational study deviates further from a target trial, rendering the marginal distribution of the observed outcomes deviate further from that of the potential outcomes. Therefore, to recover causal estimands, which are functions of potential outcomes, more sample units are required in observational studies with limited overlap.

Remark 2. For binary outcomes, because the mean of a Bernoulli distribution determines the variance, compared to the continuous outcomes in Section 3.3, we have two fewer

constraints to determine the outcome distribution. As a simple solution, we recommend to use linear models for binary outcomes so that the proposed methodology directly applies. Simulations (Section 5.2) and real applications (Section 6) later suggest that such a method generally works well in practice.

Remark 3. IPW is prone to extreme weights, which lead to inflated variance of the Hájek estimator and thus much reduced power. The common remedy is trimming, i.e. to exclusive units with extreme weights (Crump et al., 2009). However, trimming reduces the actual sample size, and more importantly, changes the target estimand to the population with substantial overlap. When extreme weights are expected, we recommend the users to consider alternative estimands targeting at the overlapped population, such as the ATO, and apply the related sample size calculation formulas developed in Section 4.

4 Weighted average treatment effect estimands

We extend the above methodology to a general class of weighted average treatment effect (WATE), which includes the ATE and several other common estimands as special cases. Averaging the CATE $\tau(x)$ over a *target population*, we obtain the average treatment effect of that population. Specifically, assume the observed sample is drawn from a population with covariates distribution $f(x)$, and let $f(x)h(x)$ denote the covariate distribution of the target population, where $h(x)$ is called a tilting function. Then we can represent the average treatment effect on the target population by a WATE

$$\tau^h = \frac{\mathbb{E}[\tau(x)h(x)]}{\mathbb{E}[h(x)]}. \quad (20)$$

When $h(x) = 1$, τ^h reduces to the ATE; when $h(x) = e(x)$, τ^h becomes the average treatment effect for the treated (ATT); when $h(x) = e(x)(1 - e(x))$, τ^h becomes the av-

erage treatment effect for the overlap population (ATO). We can use a unified weighting strategy to identify the WATE because $\tau^h = \mathbb{E}[w_1(X)ZY - w_0(X)(1 - Z)Y]$, where $w_1(x) = h(x)/e(x)$, $w_0(x) = h(x)/(1 - e(x))$ (Li et al., 2018). This corresponds to (i) the inverse probability weight, $(w_1 = 1/e(x), w_0 = 1/(1 - e(x)))$, for the ATE; (ii) the ATT weight, $(w_1 = 1, w_0 = e(x)/(1 - e(x)))$, for the ATT; and (iii) the overlap weight (OW), $(w_1 = 1 - e(x), w_0 = e(x))$, for the ATO.

The Hájek estimator for the WATE is:

$$\hat{\tau}_w = \frac{\sum_i w_1(X_i)Z_iY_i}{\sum_i w_1(X_i)Z_i} - \frac{\sum_i w_0(X_i)(1 - Z_i)Y_i}{\sum_i w_0(X_i)(1 - Z_i)}. \quad (21)$$

We can adapt the procedures in Section 3 to derive sample size calculation formulas for the ATT and ATO estimands. Specifically, the procedures to determine the propensity score and the outcome distributions remain the same, but the variance formula changes. Unlike the ATE, there is no deterministic order between the variance of the Hájek estimator with the estimated versus true propensity score for other WATE estimands (Yang and Ding, 2018). For the same reasons as with the ATE stated in Section 2, we choose to proceed with the variance with the true e .

Below we derive the variance of the Hájek estimator for the WATE with the tilting function h :

$$V_w \equiv \mathbb{V}(\hat{\tau}_w) = \frac{1}{\mathbb{E}[h(X_i)^2]} \mathbb{E} \left[\left\{ \frac{(Y_i(1) - \xi_1)^2}{e(X_i)} + \frac{(Y_i(0) - \xi_0)^2}{1 - e(X_i)} \right\} h(X_i)^2 \right], \quad (22)$$

where $\xi_z = \mathbb{E}_h[Y_i(z)] = \mathbb{E}[h(X_i)Y_i(z)]/\mathbb{E}[h(X_i)]$; the proof is relegated to Appendix A.7. For the ATE, $h(X_i) = 1$, and V_w reduces to V as in Equation 3. For the ATT and ATO, $h(X_i)$ is a function of the propensity score $e(X_i)$ and hence V_w is also fully determined by the joint distribution of $e(X_i)$ and the potential outcomes $Y_i(z)$, which can be computed via (18). However, either the ATT or the ATO has a closed-form expression of variance, but they can be computed numerically.

We outline how to compute V_w with the tilting function $h(X)$ given the parameters (μ_e, σ_e) and $(a_1, a_0, \mu_1, \mu_0, \sigma_1^2, \sigma_0^2)$. For the ATT and ATO, $h(X)$ is a function of the propensity score $e(X)$, whose distribution can be approximated by W_e . Therefore, we can also write the tilting function as $h(W_e) = \text{expit}(W_e)$ for ATT and $h(W_e) = \text{expit}(W_e)[1 - \text{expit}(W_e)]$ for ATO, such that $h(W_e)$ has approximately the same distribution as $h(X)$. Calculating the denominator $\mathbb{E}[h(X)^2] = \mathbb{E}[h(W_e)^2]$ where $W_e \sim \mathbf{N}(\mu_e, \sigma_e^2)$ involves numerically (*e.g.* Simpson's method) evaluating the following integral

$$\int_{-\infty}^{\infty} h(u)^2 \frac{1}{\sqrt{2\pi\sigma_e^2}} \exp\left(-\frac{(u - \mu_e)^2}{2\sigma_e^2}\right) du, \quad (23)$$

which is available in most statistical software. For the numerator, we show that

$$\mathbb{E}\left[\frac{(Y_i(1) - \xi_1)^2}{e(X_i)} h(X_i)^2\right] = a_1^2 \mathbb{E}\left[\left(W_e - \frac{\mathbb{E}[h(W_e)W_e]}{\mathbb{E}[h(W_e)]}\right)^2 \frac{h(W_e)^2}{\text{expit}(W_e)}\right] + \sigma_1^2 \mathbb{E}\left[\frac{h(W_e)^2}{\text{expit}(W_e)}\right], \quad (24)$$

$$\mathbb{E}\left[\frac{(Y_i(0) - \xi_0)^2}{1 - e(X_i)} h(X_i)^2\right] = a_0^2 \mathbb{E}\left[\left(W_e - \frac{\mathbb{E}[h(W_e)W_e]}{\mathbb{E}[h(W_e)]}\right)^2 \frac{h(W_e)^2}{1 - \text{expit}(W_e)}\right] + \sigma_0^2 \mathbb{E}\left[\frac{h(W_e)^2}{1 - \text{expit}(W_e)}\right], \quad (25)$$

whose proof is relegated to Appendix A.8, where all the expectation terms only involve W_e and can hence be calculated numerically by evaluating the corresponding integrals.

5 Simulation

5.1 Simulation design

Following the simulation design in Li et al. (2019), we simulate $N = 1000$ units with 10 covariates of different types. Covariates X_1 to X_4 are binary with $\text{Ber}(p)$ with $p = 0.2, 0.4, 0.6, 0.8$ respectively; $X_5 \sim \text{Unif}(0, 1)$; X_6 to X_8 follows a Poisson distribution with

mean parameters 1, 2, and 3 respectively; $X_9 \sim \text{Gamma}(2, 3)$ and $X_{10} \sim \text{Beta}(2, 3)$. We generate the treatment indicator $Z \sim \text{Ber}(\text{expit}(\beta_0 + \kappa X\beta))$, where $\beta = (1, 1, -1, 0, -2, 1, 0.5, 0, 0, 0)'$ and $\kappa \in \{0, 0.25, 0.5, 0.75, 0.9, 1\}$ is the parameter that controls the overlap between two treatment groups. For these α values, we choose $\beta_0 = \{0, -0.248, -0.489, -0.722, -0.860, -0.951\}$ accordingly so that the treatment proportion $r = \mathbb{E}[Z] = 0.5$. We then simulate the potential outcome $Y(z) \sim \mathbf{N}(X\gamma + \tau z, 4^2)$, where $\gamma = (1, 1, -1, -1, 0, -1, -1, 0, 1, 1)'$, and let the observed outcome $Y_i = Z_i Y(1) + (1 - Z_i) Y(0)$. The outcome model implies a homogeneous treatment effect $\tau = 1$ and thus the true ATE, ATT, ATO are all 1.

The overlap between two treatment groups is shown in Figure 2: $\kappa = 0$ corresponds to randomized trials; as κ increases, the overlap decreases. For each of the six simulation settings, we simulate $B = 1000$ datasets and calculate the ATE of each dataset using the Hájek estimator (2) with a 95% confidence interval, with both the true and estimated propensity scores. We then approximate the power by the proportion of the datasets where the confidence interval does not cover zero. For $\kappa \in \{0, 0.25, 0.5, 0.75, 0.9, 1\}$, which corresponds to the overlap coefficient $\phi \in \{1.00, 0.98, 0.93, 0.87, 0.84, 0.81\}$, respectively, the power with the true propensity score is 0.944, 0.931, 0.896, 0.788, 0.683, 0.612, respectively, and the power with the estimated propensity score is 0.978, 0.972, 0.943, 0.852, 0.737, 0.659, respectively. As expected, with the same sample size, decreased degree of overlap leads to much lower power.

Now we fix the calculated power as the desired level of power, and inversely solve for the sample size, which should be close to 1000. For a given simulated dataset (X, Y, Z) , we calculate the eight summary statistics $(r, \phi, E_1, E_0, S_1, S_0, R_1, R_0)$ as discussed in Section 3. The proportion of treatment, r , is calculated by the sample mean \bar{Z} , and the observed mean and variance, E_1, E_0, S_1, S_0 are calculated with values of Y on subsets $Z = 1, 0$, respectively.

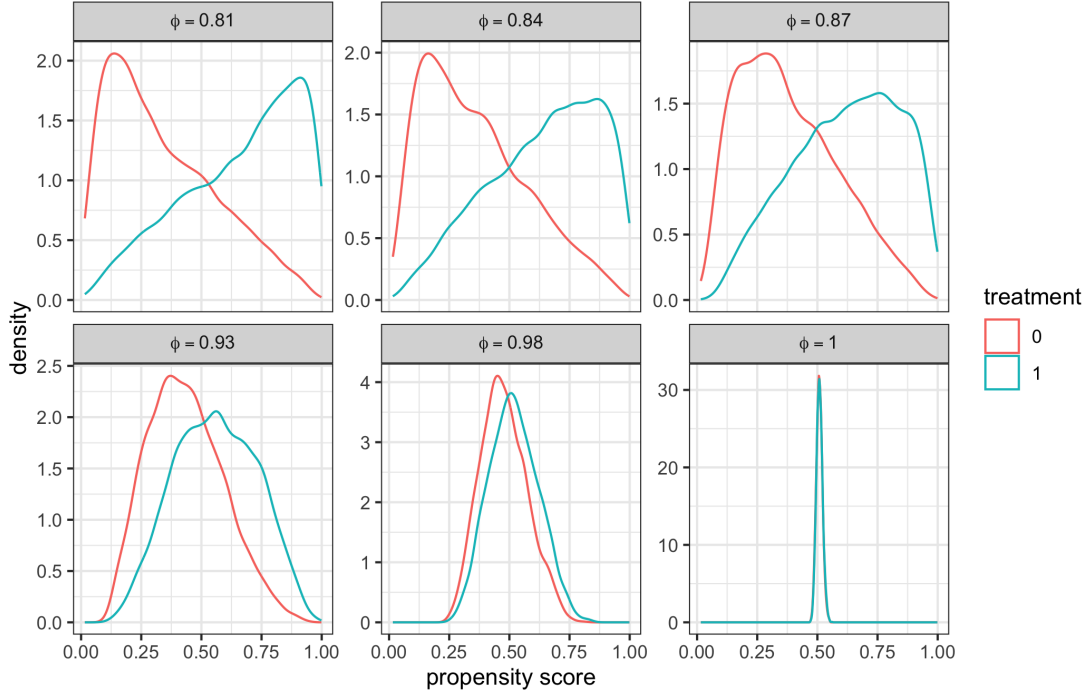


Figure 2: Distribution of the propensity scores in two treatment arms with fixed $r = 0.5$ and various overlap coefficient $\phi = 1.00, 0.98, 0.93, 0.87, 0.84, 0.81$, respectively.

With the logistic model for the propensity score, $e(X) = \text{expit}(\beta_0 + X\beta)$, the latent variable W_e is estimated by $\hat{\beta}_0 + X\hat{\beta}$, where $(\hat{\beta}_0, \hat{\beta})$ is the estimated intercept and coefficients of the logistic regression of Z on X . Although none of the covariates X is normal, the latent linear combination of X , W_e , appears to be close to normal (see the rightmost column of Figure 4 in Appendix B.1). The calculation of ϕ is more complicated, and we calculate it using the empirical CDF of the propensity scores (details are relegated to Appendix B.3). We present (r, ϕ) in Table 1 below, and the remaining quantities $(E_1, E_0, S_1, S_0, R_1, R_0)$ are shown in Table 3 in Appendix C.2.

The left side of Table 1 shows the calculated sample size to achieve the corresponding power under various degrees of overlap. The sample size to achieve nominal power of the ATE calculated with the true propensity score should theoretically be 1000, which is very close to our calculated results when overlap is good. As the overlap decreases,

ϕ	Continuous outcome				Binary outcome			
	True PS		Estimated PS		True PS		Estimated PS	
	Proposed	z -test	Proposed	z -test	Proposed	z -test	Proposed	z -test
1.00	1005	1009	1266	1275	977	977	1119	1119
0.98	992	951	1244	1202	1016	973	1162	1114
0.93	1003	827	1210	998	1036	867	1168	980
0.88	979	609	1162	719	1079	680	1153	737
0.84	980	467	1140	538	1115	543	1148	575
0.81	1065	398	1179	445	1174	460	1307	518

Table 1: Sample size calculation by the proposed method and the two-sample z -test to achieve nominal power under various degrees of overlap. The nominal power in each row is the true power of Hájek estimator for a sample of $N = 1000$ units, with true and estimated propensity scores, respectively.

the discrepancy between the calculated and the theoretical sample size increases, albeit still within a reasonable range. As noted before, the sample size calculated based on the estimated propensity scores is conservative, i.e. larger than the nominal size. The simulation results confirm this: the calculated sample size is slightly larger than the true sample size as long as the two treatment groups have a modest overlap. We also include the sample size calculated by two-sample z -test for comparison. When the overlap is perfect, the z -test correctly calculates the sample size. However, when the overlap is poor, meaning that the intended observational study is far from a target randomized trial, the z -test, which treats observational studies as randomized trials and thus ignore the degree of overlap, tends to vastly underestimate the sample size. Another observation is that the

ratio between the z -test based sample size and the nominal counterpart varies by the degree of overlap. Therefore, the existing approach of inflating the z -test based sample size with a fixed variance inflation factor (e.g. Austin, 2021) would lead to inaccurate sample sizes.

5.2 Binary outcome

We repeat the simulation design as in Section 5.1, and dichotomize the potential outcome $Y_i(z)$ into a binary variable $Y_i^b(z) = \mathbb{I}(Y_i(z) > -2)$. By SUTVA, the observed outcome $Y_i^b = Z_i Y_i^b(1) + (1 - Z_i) Y_i^b(0)$. The true ATE on Y^b is $\tau^b = \mathbb{E}[Y_i^b(1) - Y_i^b(0)] = 0.089$.

Assume we estimate τ^b using the Hájek estimator with Y_i^b . For $\kappa = \{0, 0.25, 0.5, 0.75, 0.9, 1\}$, the power with the estimated propensity scores is 0.849, 0.846, 0.797, 0.677, 0.570, 0.527, respectively, and the power with the true propensity scores is 0.798, 0.795, 0.747, 0.642, 0.546, 0.480, respectively. Dichotomizing the outcome does not affect the propensity scores, and hence (r, ϕ) remain the same as in that in Simulation 5.1. We inversely solve for the sample size, and show the results on the right side of Table 1.

The results show that the proposed method, regardless of whether the true or estimated propensity scores are used, yields sample sizes close to the nominal value 1,000. In contrast, the two-sample z -test continues to lead to vastly underestimated sample size as the degree of overlap decreases. Unlike the continuous outcome case, when the outcome is binary we tend to overestimate the sample size as the overlap coefficient decreases.

5.3 ATT and ATO estimands

With the same simulation design and data generating process as in Section 5.1, we focus on the ATT and ATO estimands, the true value of which are both 1. For $\kappa \in \{0, 0.25, 0.5, 0.75, 0.9, 1\}$, corresponding to $\phi \in \{1.00, 0.98, 0.93, 0.87, 0.84, 0.81\}$, we cal-

culate the power of the Hájek estimator (21) for the ATT and ATO, with estimated and true propensity scores, respectively. Then we inverse the process to find the sample size needed under each scenario to obtain the corresponding nominal power; the results are shown in Table 2. In all scenarios, the estimated sample size is close to the true value 1000. As predicted from the general theory on the WATE (Li et al., 2018), the ATT estimator has large variance than the ATO estimator. Consequently, given the same setting, the ATT requires larger sample size to achieve the same level of power the ATO, and the discrepancy increases as the degree of overlap decreases.

ϕ	ATT				ATO			
	True PS		Estimated PS		True PS		Estimated PS	
	Power	Size	Power	Size	Power	Size	Power	Size
1.00	0.956	1083	0.969	1178	0.936	971	0.969	1184
0.98	0.910	919	0.966	1197	0.934	988	0.966	1194
0.93	0.837	842	0.897	1026	0.920	1006	0.972	1330
0.88	0.717	854	0.711	854	0.889	959	0.923	1082
0.84	0.632	965	0.641	975	0.886	974	0.916	1085
0.81	0.593	1124	0.546	1019	0.859	912	0.904	1052

Table 2: Sample size (size) calculated by the proposed method to achieve the nominal power (power) under $r = 0.5$ and various degrees of overlap in simulations. The nominal power is the true power of Hájek estimator for a sample of $N = 1000$ units, with the true and estimated propensity scores, respectively.

As noted in Section 4, the sample size for the ATT and ATO calculated using the estimated propensity scores is not guaranteed to be conservative. However, this simulation

shows that (i) the calculated sample sizes under the true and estimated propensity scores are similar, and (ii) the sample size calculated for the ATO appears to be conservative if one expects to use the estimated propensity score in the study.

6 Real application: Right heart catheterization study

This section illustrates the proposed methods using simulations based on the right heart catheterization (RHC) observational study, a widely used benchmark dataset (Connors et al., 1996). Departing from the simulations in Section 5, here we do not impose any assumptions on the data generating model and thus provide a “fairer” assessment of the performance of our methods in real world settings. The RHC study was to evaluate the causal effect of the RHC procedure (binary treatment) among hospitalized critically ill patients. There are 5735 patients, each with 51 covariates (20 continuous, 25 binary, 6 categorical). The outcome is the binary survival status at 30 days after admission, with $Y = 1$ meaning death. In total, 2184 (38.1%) of the patients received RHC and the rest did not. The death rate is 38.0% and 30.6% in the treatment and control group, respectively. Using a logistic model with main effects of each covariate, we estimated the propensity scores and show their distributions by group in Appendix C.1 (Figure 6), suggesting a moderate degree of overlap. We numerically compute the true overlap coefficient defined in (10) to be 0.835. We also used the proposed normal approximation in Section 3.2, $W_e \sim \mathbf{N}(-0.701, 2.189)$, and estimate the overlap coefficient to be 0.822, which is close to the true value.

The Hájek estimate of the ATE is 0.066. We use bootstrap to calculate the power of the two-sided hypothesis test (4) based on the Hájek estimator. Specifically, we generate $B = 1000$ replicates, each with 5735 rows randomly drawn from the original data with

replacement. We calculate the Hájek estimate of the ATE and the associated 95% confidence interval in each replicate. Among the 1000 replicates, 983 intervals do not cover zero, giving an estimated power of 0.983 (95% CI: 0.975 to 0.991). Based on the RHC data, we compute the summary quantities $\theta = (r, \phi, E_1, E_0, S_1, S_0, R_1, R_0)$ as defined in Section 3 to be $(0.38, 0.84, 0.38, 0.31, 0.24, 0.21, 0.01, -0.02)$. The correlation $R_z = \text{cor}[Y, W_e \mid Z = z]$ is close to zero, despite that the RHC study is not a randomized trial. This could be due to the fact that the outcome is binary and thus the correlation may be misleading.

Now consider the reversed setting of sample size calculation: we want to design an observational study to replicate the RHC study. We do not have the individual data but only some summary information, based on which we calculate the sample size required to achieve the power of 0.983 with the desired effect size being 0.066. Applying the proposed method, we find that the minimal sample size is 8349, which is 45.6% larger than the actual sample size 5735. For the power values at the two endpoints of the CI, the minimal sample sizes are 7706 and 9384, respectively. There are several potential reasons for the discrepancy: (i) we used the estimated instead of the true propensity score, (ii) we treated the binary outcome as normal, and (iii) the sample size for the ATE is sensitive to minor change in power which is so close to 1. In contrast, the sample size calculated by the two-sample z -test is 3426 (95% CI: 3163 to 3851), nearly half of the actual sample size, leading to a vastly underpowered study. Given that any real study would have data attrition due to missing data and extreme weights, a conservative (overpowered) estimate of the sample size is arguably more desirable than the opposite.

We repeat the process for the ATT and ATO. The Hájek estimate of the ATT is 0.070 with power 0.966 (95% CI: 0.955 to 0.977). To achieve the power of 0.966 (0.955 to 0.977) with an effect sample size 0.070, we calculate the minimal sample size to be 4538 (4233

to 4956), which is roughly 10% below the true sample size 5735. Unlike the ATE where we overestimate the sample size, our estimate for the ATT sample size is not guaranteed conservative. For the ATO, the CIs do not cover 0 in any of the replicates, indicating that the sample is overpowered for the ATO. Therefore, we subsample 3000 rows completely at random, with which the ATO is estimated to be 0.059. Among the 1000 replicates, 895 CIs do not cover 0, leading to an estimated power of 0.895 (95% CI: 0.876 to 0.914). Reversing the process, we calculate that the sample size to be 3401 (95% CI: 3197 to 3643), which is slightly above the true sample size 3000.

Figure 3 shows the power curves of the ATE given different values of the overlap coefficient ϕ and the correlation $R_1 = R_0 = R$ while fixing other summary inputs (r, E_1, E_0, S_1, S_0) as those calculated from the RHC data. It shows that, to achieve the same power, the minimal sample size would increase as either the overlap decreases or the correlation R increases. Both patterns are as expected from the theory. The SNRs for both treatment groups are around 0.29, indicating that the absolute correlation $|R|$ is bounded within $[0, 0.46]$, which we set as the range in our power curves.

7 Discussion

This paper formulates sample size and power calculations for the propensity score analysis of causal inference with observational data. We devise theoretically justified procedures and analytical formulas to identify the three key components for sample size calculations based on commonly available and interpretable summary statistics from previous studies. We elucidate the critical role of covariate overlap between treatment groups in determining the sample size and power. Our method is applicable to continuous and binary outcomes, and the general class of weighted average treatment effect estimands that includes ATE,

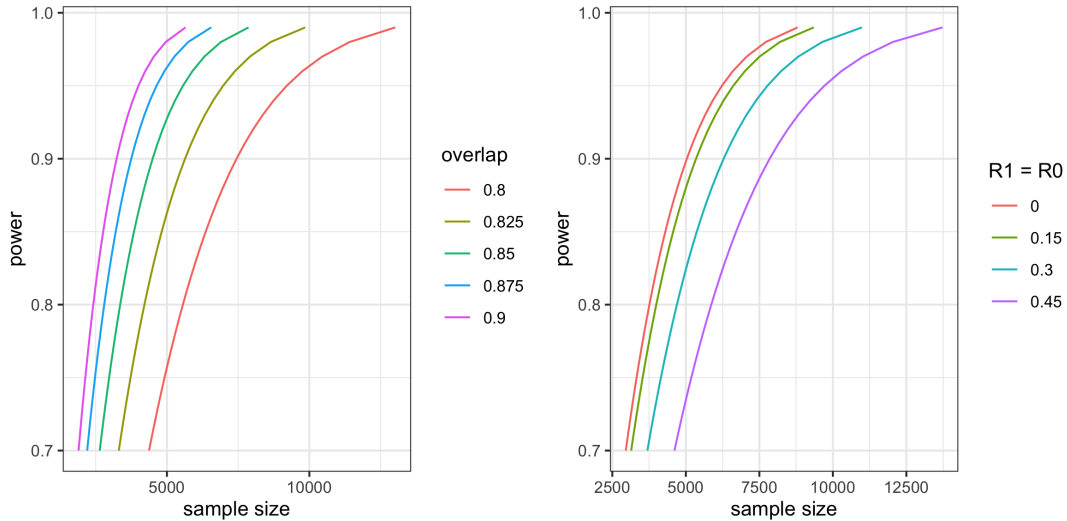


Figure 3: Power and sample size curves of an emulated RHC study with an effect size $\tau = 0.067$ under different values of the overlap coefficient ϕ (left) and the correlation $R = R_1 = R_0$ (right).

ATT, ATO. We develop the associated R package `PSpower`.

An important extension is to time-to-event outcomes. In principle, the general structure of sample size calculations and in particular the identification of the propensity score distribution in Section 3 applies to all types of outcomes. However, censoring adds complexity to the identification of the potential outcome distributions. The hazard ratio is the dominant estimand for time-to-event outcomes. It is tied to the Cox proportional hazard outcome model and its causal interpretation stands only in certain settings (Hernán, 2010). The existing literature for power calculation of multivariate Cox regression used the variance inflation approximation (Hsieh and Lavori, 2000; Scosyrev and Glimm, 2019), but it does not apply to causal analysis. A natural direction for sample size calculations of causal survival studies is to analyze the variance of the inverse probability weighted Cox model. Though closed-form solutions for the sample size calculation of the resulting marginal hazard ratio are unlikely to be available, easily computable approximations are expected to

exist following the similar structure developed in this paper.

References

- Aitchison, J. and Shen, S. M. (1980). Logistic-normal distributions: Some properties and uses. *Biometrika*, 67(2):261–272.
- Austin, P. C. (2021). Informing power and sample size calculations when using inverse probability of treatment weighting using the propensity score. *Statistics in Medicine*, 40(27):6150–6163.
- Bhattacharyya, A. (1943). On a measure of divergence between two statistical populations defined by their probability distribution. *Bulletin of the Calcutta Mathematical Society*, 35:99–110.
- Billingsley, P. (1995). *Probability and measure*. John Wiley & Sons.
- Connors, A. F., Speroff, T., Dawson, N. V., Thomas, C., Harrell, F. E., Wagner, D., Desbiens, N., Goldman, L., Wu, A. W., Califf, R. M., Fulkerson, W. J., Vidaillet, H., Broste, S., Bellamy, P., Lynn, J., and Knaus, W. A. (1996). The effectiveness of right heart catheterization in the initial care of critically ill patients. *Journal of the American Medical Association*, 276(11):889–897.
- Crump, R. K., Hotz, V. J., Imbens, G. W., and Mitnik, O. A. (2009). Dealing with limited overlap in estimation of average treatment effects. *Biometrika*, 96(1):187–199.
- Hernán, M. A. (2010). The hazards of hazard ratios. *Epidemiology*, 21(1):13.
- Hsieh, F. and Lavori, P. W. (2000). Sample-size calculations for the Cox proportional

- hazards regression model with nonbinary covariates. *Controlled clinical trials*, 21(6):552–560.
- Kelcey, B., Dong, N., Spybrook, J., and Cox, K. (2017). Statistical power for causally defined indirect effects in group-randomized trials with individual-level mediators. *Journal of Educational and Behavioral Statistics*, 42(5):499–530.
- Li, F., Morgan, K. L., and Zaslavsky, A. M. (2018). Balancing covariates via propensity score weighting. *Journal of the American Statistical Association*, 113(521):390–400.
- Li, F., Thomas, L. E., and Li, F. (2019). Addressing extreme propensity scores via the overlap weights. *American journal of epidemiology*, 188(1):250–257.
- Li, F., Zaslavsky, A. M., and Landrum, M. B. (2013). Propensity score weighting with multilevel data. *Statistics in medicine*, 32(19):3373–3387.
- Lunceford, J. K. and Davidian, M. (2004). Stratification and weighting via the propensity score in estimation of causal treatment effects: a comparative study. *Statistics in medicine*, 23(19):2937–2960.
- Qin, X. (2024). Sample size and power calculations for causal mediation analysis: a tutorial and shiny app. *Behavior Research Methods*, 56(3):1738–1769.
- Raudenbush, S. W. (1997). Statistical analysis and optimal design for cluster randomised trials. *Psychological Methods*, 2(2):173–185.
- Rosenbaum, P. R. and Rubin, D. B. (1983). The central role of the propensity score in observational studies for causal effects. *Biometrika*, 70(1):41–55.
- Scosyrev, E. and Glimm, E. (2019). Power analysis for multivariable cox regression models. *Statistics in medicine*, 38(1):88–99.

- Shen, C., Li, X., and Li, L. (2014). Inverse probability weighting for covariate adjustment in randomized studies. *Statistics in medicine*, 33(4):555–568.
- Shook-Sa, B. E. and Hudgens, M. G. (2022). Power and sample size for observational studies of point exposure effects. *Biometrics*, 78(1):388–398.
- Yang, S. and Ding, P. (2018). Asymptotic inference of causal effects with observational studies trimmed by the estimated propensity scores. *Biometrika*, 105(2):487–493.
- Zeng, S., Li, F., Wang, R., and Li, F. (2021). Propensity score weighting for covariate adjustment in randomized clinical trials. *Statistics in medicine*, 40(4):842–858.

Appendix

Appendix A. Proof of Propositions and Theorems

A.1. Proof of Proposition 1 Rewrite $\hat{\tau}_N = \tau + \epsilon\sqrt{V_0/N}$, where $\epsilon \sim \mathbf{N}(0, 1)$. Then the power of test is given by

$$\Pr\left(\tau + \epsilon\sqrt{\frac{V_0}{N}} > z_{1-\alpha}\sqrt{\frac{V}{N}}\right) = \Pr\left(\epsilon > z_{1-\alpha}\sqrt{\frac{V}{V_0}} - \tau\sqrt{\frac{N}{V_0}}\right) \quad (26)$$

$$= 1 - \Phi\left(\frac{z_{1-\alpha}\sqrt{V} - \tau\sqrt{N}}{\sqrt{V_0}}\right). \quad (27)$$

Equalizing this power with β , we obtain the sample size formula

$$N = \frac{\left(z_{1-\alpha}\sqrt{V} - z_{1-\beta}\sqrt{V_0}\right)^2}{\tau^2}. \quad (28)$$

Furthermore, when $\alpha < 0.5 < \beta$, $z_{1-\alpha} > 0$, $z_{1-\beta} < 0$, and hence we have

$$N \leq \frac{V}{\tau^2} (z_{1-\alpha} - z_{1-\beta})^2 = \frac{V}{\tau^2} (z_{1-\alpha} + z_\beta)^2. \quad (29)$$

A.2. Special case of the Lyapunov Central Limit Theorem For completeness, we first present the general form of the Lyapunov Central Limit Theorem (CLT).

Theorem (Lyapunov CLT). *Suppose $\{Z_1, \dots, Z_n, \dots\}$ is a sequence of independent random variables, each with finite expected value μ_i and variance σ_i^2 . Define $s_n^2 = \sum_{i=1}^n \sigma_i^2$. If for some $\delta > 0$, the Lyapunov's condition*

$$\lim_{n \rightarrow \infty} \frac{1}{s_n^{2+\delta}} \sum_{i=1}^n \mathbb{E} [|Z_i - \mu_i|^{2+\delta}] = 0 \quad (30)$$

is satisfied, then

$$\frac{1}{s_n} \sum_{i=1}^n (Z_i - \mu_i) \Rightarrow \mathbf{N}(0, 1). \quad (31)$$

As a special case, let $Z_i = \beta_i X_i$, where $\{X_1, \dots, X_n, \dots\}$ is a sequence of independent random variables with expectation 0 and variance 1. Then Z_i has expectation 0 and variance β_i^2 . Assume (1) $\mathbb{E}[X_i^4] \leq B < \infty$ and (2) $M_n \equiv \frac{\max_{1 \leq i \leq n} \beta_i^2}{\sum_{i=1}^n \beta_i^2} = o(1)$, then the Lyapunov's condition is satisfied (by taking $\delta = 2$) because

$$\begin{aligned} \lim_{n \rightarrow \infty} \frac{1}{(\sum_{i=1}^n \beta_i^2)^2} \sum_{i=1}^n \beta_i^4 \mathbb{E}[X_i^4] &\leq B \lim_{n \rightarrow \infty} \frac{\sum_{i=1}^n \beta_i^4}{(\sum_{i=1}^n \beta_i^2)^2} \\ &\leq B \lim_{n \rightarrow \infty} \frac{\max_{1 \leq i \leq n} \beta_i^2 \sum_{i=1}^n \beta_i^2}{(\sum_{i=1}^n \beta_i^2)^2} \\ &= B \lim_{n \rightarrow \infty} M_n \\ &= 0. \end{aligned}$$

Therefore, $\sum_{i=1}^n \beta_i X_i$ is approximately a normal distribution with mean 0 and variance $\sum_{i=1}^n \beta_i^2$ when n is large.

A.3. Proof of Proposition 2 Suppose $U \sim \text{Beta}(a, b)$ and $Z \sim \text{Bin}(U)$. Then,

$$\mathbb{E}[Z] = \mathbb{E}[\mathbb{E}[Z | U]] = \mathbb{E}[U] = \frac{a}{a+b}. \quad (32)$$

Furthermore, define $f_z(u) = \Pr(U = u | Z = z)$ for $z \in \{0, 1\}$. By Bayes' rule,

$$f_z(u) = \Pr(U = u | Z = z) = \frac{\Pr(U = u) \Pr(Z = z | U = u)}{\Pr(Z = z)}. \quad (33)$$

Therefore,

$$\begin{aligned} f_1(u) &= \frac{\Pr(U = u)u}{a/(a+b)} = \frac{\Gamma(a+b)}{\Gamma(a)\Gamma(b)} \frac{u^a(1-u)^{b-1}}{a/(a+b)} = \frac{\Gamma(a+b+1)}{\Gamma(a+1)\Gamma(b)} u^a(1-u)^{b-1}, \\ f_0(u) &= \frac{\Pr(U = u)(1-u)}{b/(a+b)} = \frac{\Gamma(a+b)}{\Gamma(a)\Gamma(b)} \frac{u^{a-1}(1-u)^b}{b/(a+b)} = \frac{\Gamma(a+b+1)}{\Gamma(a)\Gamma(b+1)} u^{a-1}(1-u)^b. \end{aligned}$$

Consequently,

$$\begin{aligned}
\phi &= \int_0^1 \sqrt{\frac{\Gamma(a+b+1)^2}{\Gamma(a+1)\Gamma(b)\Gamma(a)\Gamma(b+1)}} u^{a-0.5}(1-u)^{b-0.5} du \\
&= \frac{\Gamma(a+b+1)}{\sqrt{a}\Gamma(a)\sqrt{b}\Gamma(b)} \cdot \frac{\Gamma(a+0.5)\Gamma(b+0.5)}{\Gamma(a+b+1)} \\
&= \frac{\Gamma(a+0.5)\Gamma(b+0.5)}{\sqrt{a}\Gamma(a)\sqrt{b}\Gamma(b)}.
\end{aligned}$$

A.4. Proof of Proposition 3 Let $h(k) = \log \phi(k) = \log \Gamma\left(kr + \frac{1}{2}\right) - \log \Gamma(kr) + \log \Gamma\left(k(1-r) + \frac{1}{2}\right) - \log \Gamma(k(1-r)) - \log k - \frac{1}{2} \log(r(1-r))$. Then, it suffices to show that $h'(k) > 0$ for all k such that $2kr > 1$ and $2k(1-r) > 1$.

Denote by ψ the digamma function, $\psi(x) = (\log \Gamma(x))'$. Then,

$$h'(k) = r\psi\left(kr + \frac{1}{2}\right) - r\psi(kr) + (1-r)\psi\left(k(1-r) + \frac{1}{2}\right) - (1-r)\psi(k(1-r)) - \frac{1}{k}. \quad (34)$$

Using the equality

$$\psi(x) - \psi(y) = \int_0^1 \frac{t^{y-1} - t^{x-1}}{1-t} dt, \quad \forall x, y > 1, \quad (35)$$

we have

$$h'(k) = r \int_0^1 \frac{t^{kr-1} (1-\sqrt{t})}{1-t} dt + (1-r) \int_0^1 \frac{t^{k(1-r)-1} (1-\sqrt{t})}{1-t} dt - \frac{1}{k} \quad (36)$$

$$= \int_0^1 \frac{rt^{kr-1} + (1-r)t^{k(1-r)-1}}{1+\sqrt{t}} dt - \frac{1}{k}. \quad (37)$$

Changing variable ($t = u^2$) yields

$$h'(k) = \int_0^1 \frac{2ru^{2kr} + 2(1-r)u^{2k(1-r)}}{u(1+u)} du - \frac{1}{k} \quad (38)$$

$$= \frac{1}{k} \left\{ \int_0^1 \frac{d(u^{2kr} + u^{2k(1-r)})}{1+u} - 1 \right\} \quad (39)$$

$$= \frac{1}{k} \left\{ \frac{u^{2kr} + u^{2k(1-r)}}{1+u} \Big|_0^1 + \int_0^1 \frac{u^{2kr} + u^{2k(1-r)}}{(1+u)^2} du - 1 \right\} \quad (40)$$

$$= \frac{1}{k} \int_0^1 \frac{u^{2kr} + u^{2k(1-r)}}{(1+u)^2} du > 0. \quad (41)$$

A.5. Proof of Equation (14). Recall $Y(z) = a_z W_e + \epsilon_z$ where $\epsilon_z \sim \mathbf{N}(\mu_z, \sigma_z^2)$. The observed quantities satisfy the following equations.

$$E_z \equiv \mathbb{E}[Y \mid Z = z] = \mathbb{E}[a_z W_e + \epsilon_z \mid Z = z] = a_z \mathbb{E}[W_e \mid Z = z] + \mu_z; \quad (42)$$

$$S_z \equiv \mathbb{V}[Y \mid Z = z] = \mathbb{V}[a_z W_e + \epsilon_z \mid Z = z] = a_z^2 \mathbb{V}[W_e \mid Z = z] + \sigma_z^2; \quad (43)$$

$$R_z \equiv \text{cor}[Y, W_e \mid Z = z] = \text{cor}[a_z W_e + \epsilon_z, W_e \mid Z = z] = \frac{a_z \mathbb{V}[W_e \mid Z = z]}{\sqrt{S_z \mathbb{V}[W_e \mid Z = z]}}. \quad (44)$$

By (44),

$$a_z = \rho_z \sqrt{\frac{S_z}{\mathbb{V}[W_e \mid Z = z]}}, \quad (45)$$

which, plugged into (42) and (43), yields

$$\mu_z = E_z - a_z \mathbb{E}[W_e \mid Z = z], \quad \sigma_z^2 = (1 - R_z^2) S_z. \quad (46)$$

A.6. Proof of the analytical form of variance V in Theorem 1. Recall that

$$V = \mathbb{E} \left[\frac{\{Y(1) - \mathbb{E}[Y(1)]\}^2}{e(X)} \right] + \mathbb{E} \left[\frac{\{Y(0) - \mathbb{E}[Y(0)]\}^2}{1 - e(X)} \right], \quad (47)$$

where $e(X) = \text{expit}(W_e)$, $Y(z) = a_z W_e + \epsilon_z$, $W_e \sim \mathbf{N}(\mu_e, \sigma_e^2)$, $\epsilon_z \sim \mathbf{N}(\mu_z, \sigma_z^2)$. Therefore,

$$\mathbb{E} \left[\frac{\{Y(1) - \mathbb{E}[Y(1)]\}^2}{e(X)} \right] = \mathbb{E} \left[\frac{a_1^2 (W_e - \mu_e)^2 + \epsilon_1^2}{\text{expit}(W_e)} \right] = a_1^2 \mathbb{E} \left[\frac{(W_e - \mu_e)^2}{\text{expit}(W_e)} \right] + \sigma_1^2 \mathbb{E} \left[\frac{1}{\text{expit}(W_e)} \right], \quad (48)$$

where

$$\mathbb{E} \left[\frac{1}{\text{expit}(W_e)} \right] = \int (1 + e^{-w}) \frac{1}{\sqrt{2\pi\sigma_e^2}} \exp\left(-\frac{(w - \mu_e)^2}{2\sigma_e^2}\right) dw \quad (49)$$

$$= \int (1 + e^{-u - \mu_e}) \frac{1}{\sqrt{2\pi\sigma_e^2}} \exp\left(-\frac{u^2}{2\sigma_e^2}\right) du \quad (50)$$

$$= \int \frac{1}{\sqrt{2\pi\sigma_e^2}} \exp\left(-\frac{u^2}{2\sigma_e^2}\right) du + \int \frac{1}{\sqrt{2\pi\sigma_e^2}} \exp\left(-\frac{(u + \sigma_e^2)^2}{2\sigma_e^2} - \mu_e + \frac{\sigma_e^2}{2}\right) du \quad (51)$$

$$= 1 + \exp\left(-\mu_e + \frac{1}{2}\sigma_e^2\right), \quad (52)$$

and

$$\mathbb{E} \left[\frac{(W_e - \mu_e)^2}{\text{expit}(W_e)} \right] = \int (w - \mu_e)^2 (1 + e^{-w}) \frac{1}{\sqrt{2\pi\sigma_e^2}} \exp \left(-\frac{(w - \mu_e)^2}{2\sigma_e^2} \right) dw \quad (53)$$

$$= \int u^2 (1 + e^{-u-\mu_e}) \frac{1}{\sqrt{2\pi\sigma_e^2}} \exp \left(-\frac{u^2}{2\sigma_e^2} \right) du \quad (54)$$

$$= \int u^2 \frac{1}{\sqrt{2\pi\sigma_e^2}} \exp \left(-\frac{u^2}{2\sigma_e^2} \right) du + \int u^2 \frac{1}{\sqrt{2\pi\sigma_e^2}} \exp \left(-\frac{(u + \sigma_e^2)^2}{2\sigma_e^2} - \mu_e + \frac{\sigma_e^2}{2} \right) du \quad (55)$$

$$= \sigma_e^2 + (\sigma_e^4 + \sigma_e^2) \exp \left(-\mu_e + \frac{1}{2}\sigma_e^2 \right). \quad (56)$$

Therefore,

$$\mathbb{E} \left[\frac{\{Y(1) - \mathbb{E}[Y(1)]\}^2}{e(X)} \right] = a_1^2 \sigma_e^2 + \sigma_1^2 + [a_1^2 \sigma_e^2 (\sigma_e^2 + 1) + \sigma_1^2] \exp \left(-\mu_e + \frac{1}{2}\sigma_e^2 \right). \quad (57)$$

Similarly,

$$\mathbb{E} \left[\frac{\{Y(0) - \mathbb{E}[Y(0)]\}^2}{1 - e(X)} \right] = \mathbb{E} \left[\frac{a_0^2 (W_e - \mu_e)^2 + \epsilon_0^2}{1 - \text{expit}(W_e)} \right] = a_0^2 \mathbb{E} \left[\frac{(W_e - \mu_e)^2}{1 - \text{expit}(W_e)} \right] + \sigma_0^2 \mathbb{E} \left[\frac{1}{1 - \text{expit}(W_e)} \right], \quad (58)$$

where

$$\mathbb{E} \left[\frac{1}{1 - \text{expit}(W_e)} \right] = \int (1 + e^w) \frac{1}{\sqrt{2\pi\sigma_e^2}} \exp \left(-\frac{(w - \mu_e)^2}{2\sigma_e^2} \right) dw \quad (59)$$

$$= \int (1 + e^{u+\mu_e}) \frac{1}{\sqrt{2\pi\sigma_e^2}} \exp \left(-\frac{u^2}{2\sigma_e^2} \right) du \quad (60)$$

$$= \int \frac{1}{\sqrt{2\pi\sigma_e^2}} \exp \left(-\frac{u^2}{2\sigma_e^2} \right) du + \int \frac{1}{\sqrt{2\pi\sigma_e^2}} \exp \left(-\frac{(u - \sigma_e^2)^2}{2\sigma_e^2} + \mu_e + \frac{\sigma_e^2}{2} \right) du \quad (61)$$

$$= 1 + \exp \left(\mu_e + \frac{1}{2}\sigma_e^2 \right), \quad (62)$$

and

$$\mathbb{E} \left[\frac{(W_e - \mu_e)^2}{1 - \text{expit}(W_e)} \right] = \int (w - \mu_e)^2 (1 + e^w) \frac{1}{\sqrt{2\pi\sigma_e^2}} \exp \left(-\frac{(w - \mu_e)^2}{2\sigma_e^2} \right) dw \quad (63)$$

$$= \int u^2 (1 + e^{u+\mu_e}) \frac{1}{\sqrt{2\pi\sigma_e^2}} \exp \left(-\frac{u^2}{2\sigma_e^2} \right) du \quad (64)$$

$$= \int u^2 \frac{1}{\sqrt{2\pi\sigma_e^2}} \exp \left(-\frac{u^2}{2\sigma_e^2} \right) du + \int u^2 \frac{1}{\sqrt{2\pi\sigma_e^2}} \exp \left(-\frac{(u - \sigma_e^2)^2}{2\sigma_e^2} + \mu_e + \frac{\sigma_e^2}{2} \right) du \quad (65)$$

$$= \sigma_e^2 + (\sigma_e^4 + \sigma_e^2) \exp \left(\mu_e + \frac{1}{2}\sigma_e^2 \right). \quad (66)$$

Therefore,

$$\mathbb{E} \left[\frac{\{Y(0) - \mathbb{E}[Y(0)]\}^2}{1 - e(X)} \right] = a_0^2 \sigma_e^2 + \sigma_0^2 + [a_0^2 \sigma_e^2 (\sigma_e^2 + 1) + \sigma_0^2] \exp \left(\mu_e + \frac{1}{2}\sigma_e^2 \right). \quad (67)$$

Adding (57) and (67), we have

$$V = (a_1^2 + a_0^2) \sigma_e^2 + (\sigma_1^2 + \sigma_0^2) + [a_1^2 \sigma_e^2 (\sigma_e^2 + 1) + \sigma_1^2] \exp \left(-\mu_e + \frac{1}{2}\sigma_e^2 \right) + [a_0^2 \sigma_e^2 (\sigma_e^2 + 1) + \sigma_0^2] \exp \left(\mu_e + \frac{1}{2}\sigma_e^2 \right). \quad (68)$$

A.7. Proof of the asymptotic variance of the general Hájek WATE estimator.

Let

$$\xi_1^* = \frac{\mathbb{E}[h(X_i; \alpha^*) Y_i(1)]}{\mathbb{E}[h(X_i; \alpha^*)]}, \quad \xi_0^* = \frac{\mathbb{E}[h(X_i; \alpha^*) Y_i(0)]}{\mathbb{E}[h(X_i; \alpha^*)]}$$

be the expected potential outcomes given the tilting function $h(x)$ and let α^* be the true parameter value for the propensity score model $e(X; \alpha)$. Let

$$\hat{\xi}_1 = \frac{\sum_{i=1}^N Z_i Y_i \hat{w}_1(X_i)}{\sum_{i=1}^N Z_i \hat{w}_1(X_i)}, \quad \hat{\xi}_0 = \frac{\sum_{i=1}^N (1 - Z_i) Y_i \hat{w}_0(X_i)}{\sum_{i=1}^N (1 - Z_i) \hat{w}_0(X_i)},$$

and

$$\hat{\tau}_w = \hat{\xi}_1 - \hat{\xi}_0.$$

Then $(\hat{\xi}_1, \hat{\xi}_0, \hat{\alpha})$ jointly solves

$$0 = \frac{1}{N} \sum_{i=1}^N \phi(Y_i(1), Y_i(0), x_i, Z_i; \xi_1, \xi_0, \alpha) = \frac{1}{N} \sum_{i=1}^N \begin{pmatrix} \phi_1(Y_i(1), x_i, Z_i; \xi_1, \alpha) \\ \phi_0(Y_i(0), x_i, Z_i; \xi_0, \alpha) \\ \psi_\alpha(x_i, Z_i; \alpha) \end{pmatrix}$$

where

$$\phi = \begin{pmatrix} \phi_1 \\ \phi_0 \\ \psi_\alpha \end{pmatrix} \quad \text{with} \quad \begin{aligned} \phi_1 &= Z_i \cdot w_1(X_i; \alpha) \cdot \{Y_i(1) - \xi_1\}, \\ \phi_0 &= (1 - Z_i) \cdot w_0(X_i; \alpha) \cdot \{Y_i(0) - \xi_0\}, \\ \psi_\alpha &= e'(X_i; \alpha) \{Z_i - e(X_i; \alpha)\}. \end{aligned} \quad (69)$$

It is straightforward to verify that $\mathbb{E}[\phi(\xi_1^*, \xi_0^*, \alpha^*)] = 0$. The theory of M-estimation states that

$$\sqrt{N} \begin{pmatrix} \hat{\xi}_1 - \xi_1^* \\ \hat{\xi}_0 - \xi_0^* \\ \hat{\alpha} - \alpha^* \end{pmatrix} \xrightarrow{d} \mathcal{N}(0, (A^*)^{-1} B^* (A^*)^{-\top}), \quad (70)$$

where A^* and B^* are the values of $-\mathbb{E}\left(\frac{\partial \phi}{\partial(\xi_1, \xi_0, \alpha)}\right)$ and $\mathbb{E}[\phi \phi^\top]$ evaluated at $(\xi_1^*, \xi_0^*, \alpha^*)$ respectively.

Calculation of A^* . By definition, we have

$$\frac{\partial \phi}{\partial(\xi_1, \xi_0, \alpha)} \Big|_{(\xi_1^*, \xi_0^*, \alpha^*)} = \begin{pmatrix} \frac{\partial \phi_1^*}{\partial \xi_1} & 0 & \frac{\partial \phi_1^*}{\partial \alpha^\top} \\ 0 & \frac{\partial \phi_0^*}{\partial \xi_0} & \frac{\partial \phi_0^*}{\partial \alpha^\top} \\ 0 & 0 & \frac{\partial \psi_\alpha^*}{\partial \alpha^\top} \end{pmatrix} \quad (71)$$

where

$$\begin{aligned}
\frac{\partial \phi_1^*}{\partial \xi_1} &= -Z_i \cdot w_1(X_i; \alpha^*), \\
\frac{\partial \phi_0^*}{\partial \xi_0} &= -(1 - Z_i) \cdot w_0(X_i; \alpha^*), \\
\frac{\partial \phi_1^*}{\partial \alpha} &= Z_i \cdot \{Y_i(1) - \xi_1^*\} \cdot w_1'(X_i; \alpha^*), \\
\frac{\partial \phi_0^*}{\partial \alpha} &= (1 - Z_i) \cdot \{Y_i(0) - \xi_0^*\} \cdot w_0'(X_i; \alpha^*), \\
\frac{\partial \psi_\alpha^*}{\partial \alpha} &= e''(X_i; \alpha^*)(Z_i - e(X_i; \alpha^*)) - [e'(X_i; \alpha^*)][e'(X_i; \alpha^*)]^\top.
\end{aligned}$$

Accordingly, we have

$$A^* = \begin{pmatrix} a_{11} & 0 & a_{13} \\ 0 & a_{22} & a_{23} \\ 0 & 0 & a_{33} \end{pmatrix},$$

where

$$a_{11} = \mathbb{E}[Z_i \cdot w_1(X_i; \alpha^*)] = \mathbb{E}[e(X_i; \alpha^*)w_1(X_i; \alpha^*)] = \mathbb{E}[h(X_i; \alpha^*)],$$

$$a_{22} = \mathbb{E}[(1 - Z_i) \cdot w_0(X_i; \alpha^*)] = \mathbb{E}[(1 - e(X_i; \alpha^*))w_0(X_i; \alpha^*)] = \mathbb{E}[h(X_i; \alpha^*)],$$

$$a_{13} = \mathbb{E}[-Z_i \cdot \{Y_i(1) - \xi_1^*\} \cdot w_1'(X_i; \alpha^*)] = -\mathbb{E}[e(X_i; \alpha^*) \cdot \{Y_i(1) - \xi_1^*\} \cdot w_1'(X_i; \alpha^*)],$$

$$a_{23} = \mathbb{E}[-(1 - Z_i) \cdot \{Y_i(0) - \xi_0^*\} \cdot w_0'(X_i; \alpha^*)] = -\mathbb{E}[(1 - e(X_i; \alpha^*)) \cdot \{Y_i(0) - \xi_0^*\} \cdot w_0'(X_i; \alpha^*)],$$

$$a_{33} = \mathbb{E}[-e'(X_i; \alpha^*)e'(X_i; \alpha^*)^\top].$$

Calculation of B^* .

$$B^* = \mathbb{E}[\phi^* \phi^{*\top}] = \begin{pmatrix} b_{11} & 0 & b_{13} \\ 0 & b_{22} & b_{23} \\ b_{13}^\top & b_{23}^\top & b_{33} \end{pmatrix},$$

where

$$\begin{aligned}
b_{11} &= \mathbb{E} [Z_i \cdot \{Y_i(1) - \xi_1^*\}^2 \cdot w_1(X_i; \alpha^*)^2] = \mathbb{E} [\{Y_i(1) - \xi_1^*\}^2 e(X_i; \alpha^*) w_1(X_i; \alpha^*)^2], \\
b_{22} &= \mathbb{E} [(1 - Z_i) \cdot \{Y_i(0) - \xi_0^*\}^2 \cdot w_0(X_i; \alpha^*)^2] = \mathbb{E} [\{Y_i(0) - \xi_0^*\}^2 \{1 - e(X_i; \alpha^*)\} w_0(X_i; \alpha^*)^2], \\
b_{13} &= \mathbb{E} [Z_i (Z_i - e(X_i; \alpha^*)) \cdot w_1(X_i; \alpha^*) \cdot \{Y_i(1) - \xi_1^*\} \cdot e'(X_i; \alpha^*)] \\
&= \mathbb{E} [e(X_i; \alpha^*) \{1 - e(X_i; \alpha^*)\} \cdot w_1(X_i; \alpha^*) \cdot \{Y_i(1) - \xi_1^*\} \cdot e'(X_i; \alpha^*)], \\
b_{23} &= \mathbb{E} [(1 - Z_i) (Z_i - e(X_i; \alpha^*)) \cdot w_0(X_i; \alpha^*) \cdot \{Y_i(0) - \xi_0^*\} \cdot e'(X_i; \alpha^*)] \\
&= \mathbb{E} [-e(X_i; \alpha^*) \{1 - e(X_i; \alpha^*)\} \cdot w_0(X_i; \alpha^*) \cdot \{Y_i(0) - \xi_0^*\} \cdot e'(X_i; \alpha^*)], \\
b_{33} &= \mathbb{E} [e(X_i; \alpha^*) \{1 - e(X_i; \alpha^*)\} e'(X_i; \alpha^*) e'(X_i; \alpha^*)^\top].
\end{aligned}$$

Calculation of $(A^*)^{-1} B^* (A^*)^{-\top}$. First, we notice that

$$A^* = \begin{pmatrix} a_{11} & 0 & a_{13} \\ 0 & a_{11} & a_{23} \\ 0 & 0 & a_{33} \end{pmatrix} \implies (A^*)^{-1} = \begin{pmatrix} a_{11}^{-1} & 0 & -a_{11}^{-1} a_{13} a_{33}^{-1} \\ 0 & a_{11}^{-1} & -a_{11}^{-1} a_{23} a_{33}^{-1} \\ 0 & 0 & a_{33}^{-1} \end{pmatrix}$$

Therefore,

$$\begin{aligned}
(A^*)^{-1} B^* (A^*)^{-\top} &= \begin{pmatrix} a_{11}^{-1} & 0 & -a_{11}^{-1} a_{13} a_{33}^{-1} \\ 0 & a_{11}^{-1} & -a_{11}^{-1} a_{23} a_{33}^{-1} \\ 0 & 0 & a_{33}^{-1} \end{pmatrix} \begin{pmatrix} b_{11} & 0 & b_{13} \\ 0 & b_{22} & b_{23} \\ b_{13}^\top & b_{23}^\top & b_{33} \end{pmatrix} \begin{pmatrix} a_{11}^{-1} & 0 & 0 \\ 0 & a_{11}^{-1} & 0 \\ -a_{33}^{-1} c_{13}^\top a_{11}^{-1} & -a_{33}^{-1} c_{23}^\top a_{11}^{-1} & a_{33}^{-1} \end{pmatrix} \\
&= a_{11}^{-2} \begin{pmatrix} b_{11} - 2a_{13} a_{33}^{-1} b_{13}^\top + a_{13} a_{33}^{-1} a_{13}^\top & -a_{13} a_{33}^{-1} b_{23}^\top - b_{13} a_{33}^{-1} a_{23}^\top + a_{13} a_{33}^{-1} a_{23}^\top & * \\ -a_{13} a_{33}^{-1} b_{23}^\top - b_{13} a_{33}^{-1} a_{23}^\top + a_{13} a_{33}^{-1} a_{23}^\top & b_{22} - 2a_{23} a_{33}^{-1} b_{23}^\top + a_{23} a_{33}^{-1} a_{23}^\top & * \\ * & * & * \end{pmatrix}.
\end{aligned}$$

Hence,

$$\begin{aligned}
\text{Var}(\hat{\tau}_w) &= \begin{pmatrix} 1 & -1 & 0 \end{pmatrix} (A^*)^{-1} B^* (A^*)^{-\top} \begin{pmatrix} 1 \\ -1 \\ 0 \end{pmatrix} \\
&= a_{11}^{-2} [(b_{11} + b_{22} - 2(a_{13} - a_{23}) a_{33}^{-1} (b_{13} - b_{23})^\top + (a_{13} - a_{23}) a_{33}^{-1} (a_{13} - a_{23})^\top)].
\end{aligned}$$

A.8. Proof of (24) Recall that $Y(z) = a_z W_e + \epsilon_z$, where $\epsilon_z \sim \mathbf{N}(\mu_z, \sigma_z^2)$. Then,

$$\xi_z = \frac{\mathbb{E}[h(X)Y(z)]}{\mathbb{E}[h(X)]} = a_z \frac{\mathbb{E}[h(W_e)W_e]}{\mathbb{E}[h(W_e)]} + \frac{\mathbb{E}[h(W_e)\epsilon_z]}{\mathbb{E}[h(W_e)]} = a_z \frac{\mathbb{E}[h(W_e)W_e]}{\mathbb{E}[h(W_e)]} + \mu_z. \quad (72)$$

The last equation holds because ϵ_z and W_e are uncorrelated normal random variables and thus independent. Then,

$$\mathbb{E} \left[\frac{(Y_i(1) - \xi_1)^2}{e(X_i)} h(X_i)^2 \right] = \mathbb{E} \left[\left\{ a_1 \left(W_e - \frac{\mathbb{E}[h(W_e)W_e]}{\mathbb{E}[h(W_e)]} \right) + \epsilon_1 - \mu_1 \right\}^2 \frac{h(W_e)^2}{\text{expit}(W_e)} \right] \quad (73)$$

$$= \mathbb{E} \left[\mathbb{E} \left[\left\{ a_1 \left(W_e - \frac{\mathbb{E}[h(W_e)W_e]}{\mathbb{E}[h(W_e)]} \right) + \epsilon_1 - \mu_1 \right\}^2 \frac{h(W_e)^2}{\text{expit}(W_e)} \mid W_e \right] \right] \quad (74)$$

$$= \mathbb{E} \left[\left\{ a_1^2 \left(W_e - \frac{\mathbb{E}[h(W_e)W_e]}{\mathbb{E}[h(W_e)]} \right)^2 + \sigma_1^2 \right\} \frac{h(W_e)^2}{\text{expit}(W_e)} \right] \quad (75)$$

$$= a_1^2 \mathbb{E} \left[\left(W_e - \frac{\mathbb{E}[h(W_e)W_e]}{\mathbb{E}[h(W_e)]} \right)^2 \frac{h(W_e)^2}{\text{expit}(W_e)} \right] + \sigma_1^2 \mathbb{E} \left[\frac{h(W_e)^2}{\text{expit}(W_e)} \right]. \quad (76)$$

Similarly,

$$\mathbb{E} \left[\frac{(Y_i(0) - \xi_0)^2}{1 - e(X_i)} h(X_i)^2 \right] = a_0^2 \mathbb{E} \left[\left(W_e - \frac{\mathbb{E}[h(W_e)W_e]}{\mathbb{E}[h(W_e)]} \right)^2 \frac{h(W_e)^2}{1 - \text{expit}(W_e)} \right] + \sigma_0^2 \mathbb{E} \left[\frac{h(W_e)^2}{1 - \text{expit}(W_e)} \right]. \quad (77)$$

Appendix B Examples

B.1. Normality of linear combination of covariates. We consider the simulated data in Section 5 and three real world datasets: (i) RHC; (ii) the Best Apnea Interventions for Research (BestAIR) trial, a individually randomized trial with 169 units, with 9 continuous or binary covariates; more details can be found in Zeng et al. (2021); (iii) HSR: an observational study on the racial disparities of breast cancer screening, with 56,480 units and 17 binary covariates; more details can be found in Li et al. (2013). For each dataset,

we fit a simple logistic model to estimate the propensity score $e(X) = \text{expit}(\beta_0 + X'\beta)$, and we provide the density plot and Q-Q plot in Figure 4.

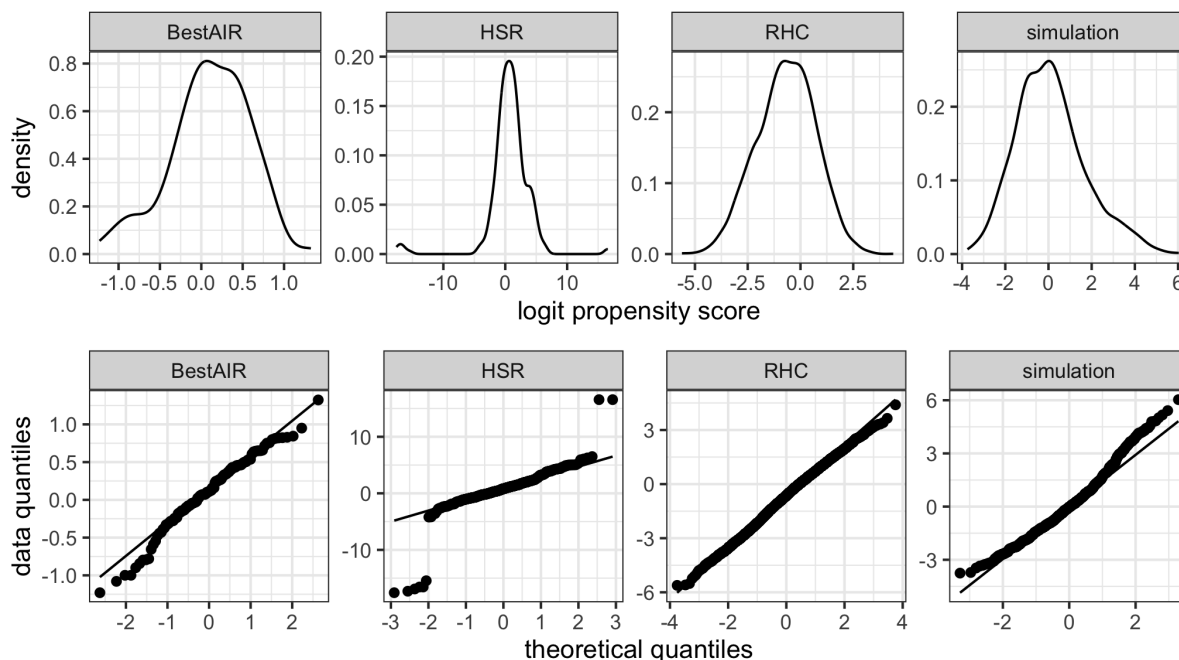


Figure 4: Density plot and Q-Q plot of fitted logit propensity scores, which is a linear combination of covariates. The proximity of the points to the reference line in the Q-Q plot shows the closeness of the distribution to a normal distribution.

B.2. Examples of the Beta approximation of logit-normal distribution. Figure 5 presents the density of the Beta distribution over a grid of (α, β) values within $\{0.5, 1, 2, 3\}$, and the density of the corresponding approximated logit-normal distributions.

B.3 Calculation of overlap coefficient ϕ with fitted propensity scores In real applications, researchers do not have access to data and thus cannot calculate ϕ with fitted propensity scores. Nevertheless, we provide a computation method here for interested

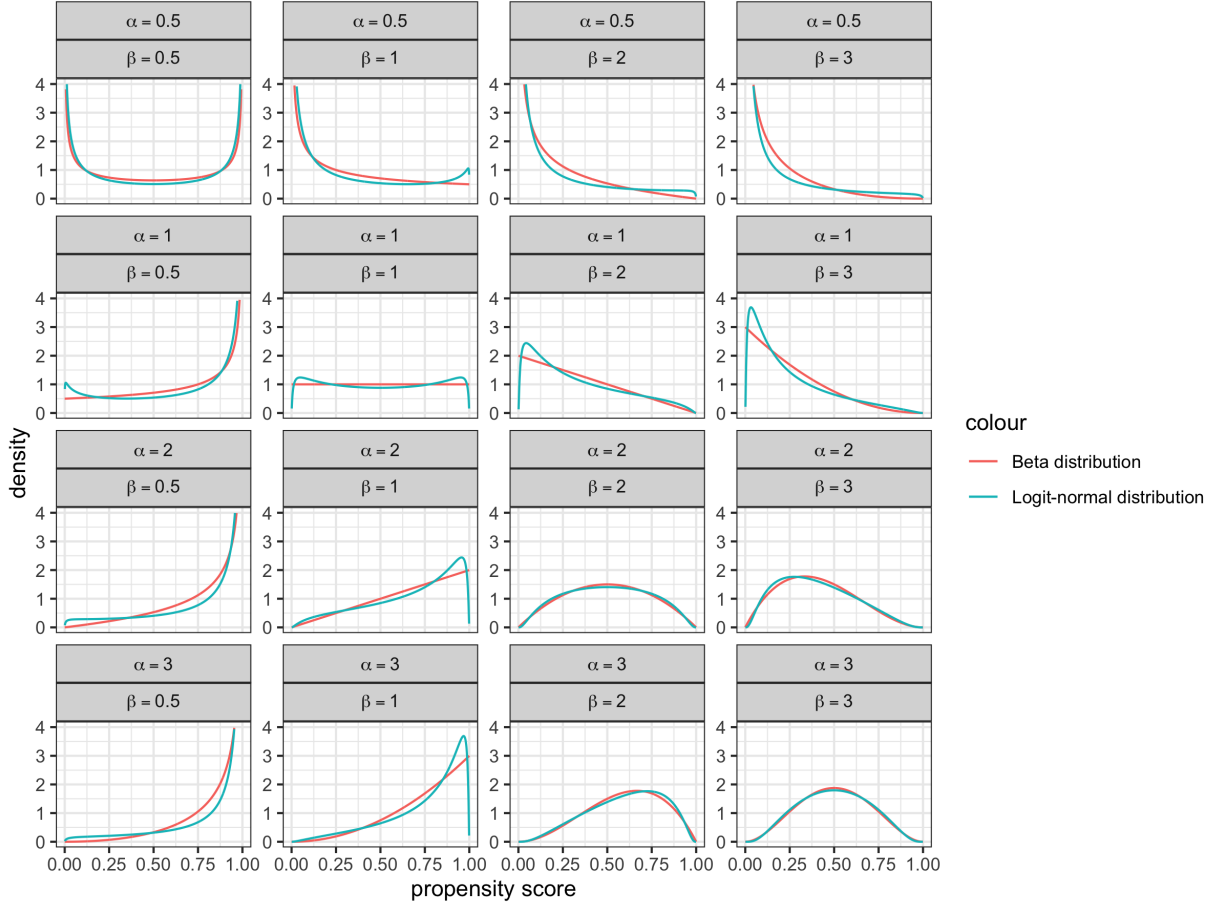


Figure 5: Examples of Beta approximation to logit-normal distribution

readers. This method is more robust than directly estimating the density and can be useful for simulation studies.

By Bayes' theorem,

$$f_z(u) = \Pr(e(X) = u \mid Z = z) = \frac{\Pr(Z = z \mid e(X) = u) \Pr(e(X) = u)}{\Pr(Z = z)}. \quad (78)$$

Hence,

$$\phi = \int_0^1 \sqrt{f_0(u) f_1(u)} du = \frac{\int_0^1 \sqrt{u(1-u)} \Pr(e(X) = u) du}{\sqrt{r(1-r)}}. \quad (79)$$

Let $F(u) = \Pr(e(X) \leq u)$ be the CDF of $e(X)$. Let $\hat{e}_1, \hat{e}_2, \dots, \hat{e}_n$ be the estimated propensity scores of the units, and let $\hat{F}(u) = \frac{1}{n} \sum_{i=1}^n \mathbb{I}(\hat{e}_i \leq u)$ be the empirical CDF of $e(X)$.

Then,

$$\phi = \frac{\int_0^1 \sqrt{u(1-u)} dF(u)}{\sqrt{r(1-r)}} \approx \frac{\int_0^1 \sqrt{u(1-u)} d\hat{F}(u)}{\sqrt{r(1-r)}} = \frac{1}{n} \cdot \frac{\sum_{i=1}^n \sqrt{\hat{e}_i(1-\hat{e}_i)}}{\sqrt{r(1-r)}}. \quad (80)$$

Appendix C. Additional Simulation and RHC Study Results

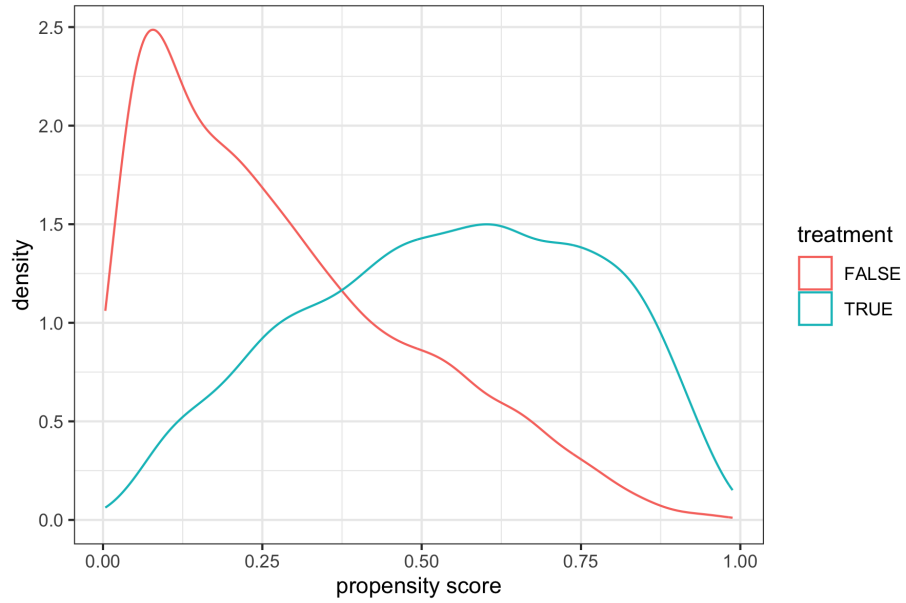


Figure 6: Density plot of the estimated propensity scores by treatment arm in RHC.

C.1. Density plot of the estimated propensity scores in the RHC study.

C.2. Summary quantities in Simulation 5.1

κ	0	0.25	0.5	0.75	0.9	1
ϕ	1.00	0.98	0.93	0.87	0.84	0.81
r	0.50	0.50	0.50	0.50	0.50	0.50
E_1	-1.74	-1.88	-2.04	-2.14	-2.13	-2.18
E_0	-2.74	-2.58	-2.41	-2.32	-2.30	-2.27
S_1	19.86	20.53	20.41	20.41	20.37	20.53
S_0	20.12	19.94	19.60	19.12	19.34	19.22
R_1	0.14	-0.20	-0.21	-0.20	-0.19	-0.20
R_0	0.14	-0.19	-0.16	-0.14	-0.13	-0.13

Table 3: Summary quantities $(r, \phi, E_1, E_0, S_1, S_0, R_1, R_0)$ under different values of κ in Simulation 5.1.